APPENDIX A: VIBRATION ASSESSMENT FOR THE RCS PIPING AND THE PIPING ATTACHED TO THE RSG

A.1 Scope

The vibration assessment for piping follows the recommendations of References 1, 10 through 13, 15, and 17. The scope of the piping for this program conforms to the guidance of Reference 15:

- ASME Code Classes 1, 2, and 3 systems.
- Other high-energy piping systems inside Seismic Category I structures.
- High energy portions of systems whose failure could reduce the functioning of any Seismic Category I plant feature to an unacceptable level.
- Seismic Category I portions of moderate energy piping systems located outside containment.

A.2 Flow-Excited Acoustic Resonance

A.2.1 Screening Methodology for Flow Excited Acoustics

Using the screening methods described in this section, ASME Code Classes 1, 2, and 3 piping will be designed so that the generation of the sources of flow excitation in the cavities of safety relief valves, standoff pipes for valves, and branch lines is not credible.

The screening methodology will be incorporated into the design of piping and valve components to preclude the possibility of the shear wave resonance coupled with acoustic resonance from occurring. This coupled phenomenon is called shear wave resonance in this Appendix. For standoff piping with the potential for acoustic resonance as identified by the Strouhal number in Reference 17, design measures for mitigation of the acoustic resonance will be taken.

Shear wave resonance of valve cavities occurs when the standing acoustic wave in the valve's cavity couples with the vortices shedding off of the leading edge of the valve cavity's mouth (See Figure A-1). When the vortex shedding frequency becomes close, or equal, to the acoustic frequency of the cavity, then high oscillating pressures may develop. The resulting resonance pressure-flow oscillation can travel through the entire affected piping system with little attenuation. The oscillating pressure amplitudes inside the valve can be much greater than the main piping line dynamic pressure. For example, in Reference 13, pressure oscillations of up to 200 psi peak to peak have been measured in the relief valve standpipes. If there are acoustic instabilities in the flow fields which resonate with the structural natural frequencies of the RCS internal components, such as in the steam generator, then sinusoidal dynamic loads can be created that may result in high cycle fatigue failure as discussed in Reference 1.

A typical method of predicting conditions conducive to shear wave resonance in piping systems and an explanation of these phenomena is presented in Reference 13. As noted in

Reference 13, flow past a standoff pipe or relief valves will separate near the leading edge forming a shear layer downstream.

The flow-induced oscillations in terms of the non-dimensional frequency can be expressed in an analytical form as shown below.

Equation 1: $f = \frac{SU}{d}$

Where:

f = frequency (Hz).

S = Strouhal Number.

U = free stream velocity.

d = diameter of the branch.

These alternating flows into and out of the cavity result in compression of the vertical column and will excite the acoustic depth modes with the frequency defined as follows:

Equation 2: $f = \frac{NC}{4L}$

Where:

N = acoustic mode number = 1, 3, 5.

C = acoustic velocity in flowing stream.

L = stub length (or the standpipe height for safety relief valves).

When the vortex shedding excitation frequency and the first acoustic modal frequency coincide, an acoustic resonance condition is created that is physically observed to be a loud noise. Equating these two frequencies and solving for the Strouhal number, the following expression is obtained:

Equation 3: $S = \frac{Cd}{4LU}$

These pulsations can be further amplified if the standpipe acoustic mode is coupled with an acoustic mode of the main piping, with velocity anti-node near the side branch entrance. In that case, the acoustic impedances will match and the side branch resonance will couple with the main pipe resonance. This scenario may cause significant vibration of the safety relief valves or other structures in the piping systems if their structural natural frequencies are coincident with the acoustic and vortex-shedding frequencies. This condition may also cause safety relief valves to

leak and chatter. Conversely, if the side branch is located near a main piping velocity node (pressure maximum), an impedance mismatch occurs and the stub standing wave will attenuate.

Baldwin and Simmons (Reference 13) evaluated plant data for safety and relief valves installed in plants and concluded that the lowest Strouhal number for which no coupling should occur is about 0.6. More recent studies by Ziada and Shine (Reference 17) indicated that no coupling should occur for a Strouhal number of 0.62 and above. The difference between these two is that Baldwin and Simmons focused on single side branches on a pipe, whereas Ziada and Shine extended the work to include the interactions between a small set of piping components and configurations. The Ziada and Shine study involved more detailed configurations that included a side branch just downstream of an elbow, two side branches on the same side of the pipe and two side branches opposite each other. It is noted that Ziada and Shine found that the Strouhal number above which resonance was not observed was 0.62 and the value of 0.63 is used for conservatism.

Substituting U/C = M (Mach number) into the expression for the Strouhal number and setting the Strouhal number equal to 0.63 yields the following design relationship, where acoustic resonance conditions will not occur. The Mach number is a function of the fluid composition, state point and local free stream velocity:

Equation 4: $$\frac{d}{L} > 4\frac{U}{C}S = 2.52M$$

The maximum allowable length-to-diameter ratio of the cavity is defined by the Mach number of the flow past the side branch. By following this design criterion, a Strouhal number of no less than 0.63 is maintained for maximum flow velocity for plant operating conditions.

Additional research (Reference 16) indicates the blend radius (r) at the mouth of the cavity is also important, depending on the forged piping connection being a sweepolet, vesselet, or other type: the critical flow velocity scales with blend radius (r) + standpipe inside diameter (d). The modified diameter (d+ r) can be viewed to be the equivalent "d" after the blend radius is taken into consideration. Therefore, Equation 1 can be further refined as:

Equation 5: $$f = \frac{SU}{(d+r)}$$

Evaluation of standoff pipes for the valves, standoff branch lines, or other cavities that have the potential to create acoustic resonance are evaluated as part of the design process for these piping systems. Appropriate design considerations are incorporated into the piping design to prevent such acoustic resonance from occurring.

A.2.2 Control Valve and Operator in Resonance

Another type of acoustic resonance is a control valve with a downstream acoustic mode as described in Reference 14. This may be prevented by verifying that the natural frequency of the control valve and operator is not near an acoustic resonance frequency of the downstream piping by design or by providing damping as shown in Reference 14.

A.2.3 Identification of Acoustic Resonance by Testing

A.2.3.1 Acoustic Resonance Caused by Flow Past Standpipes

Acoustic resonance of a standpipe or other dead leg on a system is distinctive and readily noted, as experience indicates. As described in Reference 13, the distinguishing characteristics of this resonance are pure-tone, single frequency, high amplitude excitation in a flow rate range at a frequency in excess of 100 Hertz. Frequency is related to a fraction of a wavelength of a closed-end branch line. Amplitude changes rapidly with flow rate, with amplitude increasing as a flow rate is approached from above or below. The flow rate is determined by the acoustic resonance frequency of the branch line, the flow rate past the entrance, and the diameter of the entrance. The amplitude is not decreased significantly over piping lengths typical of a power plant.

If acoustic resonance is identified in a piping system during pre-operational testing, the source will be identified using the distinguishing characteristics, and measures will be taken to mitigate resonance.

A.2.3.2 Acoustic Resonance Caused by Control Valve and Operator

Another type of acoustic resonance is a control valve with a downstream acoustic mode as described in Reference 14. This may be prevented by verifying that the natural frequency of the control valve is not near an acoustic resonance frequency of the downstream piping by design or by providing damping as shown in Reference 14. The distinguishing characteristics of this type of acoustic resonance are similar to those of acoustic resonance past a closed end branch line as described above except that the frequency is lower, typically below 30 Hertz.

A.2.3.3 Acoustic Resonance Detection Method

A monitoring system is placed on representative piping trains that are most likely to develop acoustic resonance. Sensitivity to acoustic resonance determination is based on detailed analysis, considering Strouhal numbers and other pertinent acoustic factors as outlined in the Section A.2.1.

Monitoring is not required for other piping trains that are essentially the same. The following criteria must be satisfied to qualify the piping as essentially the same:

- Part of the same overall plant system (e.g., main steam system).
- Have the same components and pipe routing, particularly for branch piping, and distances within tolerances typical of piping classes. The distance to the upstream elbow and distance

between standpipes do impact acoustic resonance phenomenon due to impact on Strouhal numbers, frequencies as well as amplitudes of standing waves as the result of interference. In order to keep piping systems tuned to comparable acoustic behavior, the allowable deviations of distances is based on construction tolerances of the piping system.

- Main piping must have the same diameter within tolerances typical of piping classes, and flow conditions within two percent of the design conditions. The flow conditions of piping system lines are considered "essentially the same" when they are within two percent of the design conditions because these affect the flow field past the entrance to branch piping.
- Have the same distance between the first upstream elbow and the standpipes, within tolerances typical of piping classes. The orientation of elbows relative to the branch line does not impact the propagation of acoustic waves or effects of acoustic wave reflections. However, the orientation of elbows is a criterion for determining similarity of pipe systems (Reference 17).
- Branch piping must have the same length and diameter within the systems, within tolerances typical of piping classes. The diameter should be within tolerances typical of piping classes.

This monitoring system is designed to detect a well-established standing wave. Therefore, the method is limited to high coherence of signals between pressure stations. The symmetrically circumferential strain gauges are designed to cancel out lobalar shell modes of vibration. Therefore, the frequency range of applicability is well below the "breathing" shell mode of the pipe. Therefore, the deformation of the pipe, as measured by the strain gauges is caused by pressure inside the pipe. The frequency limit is approximately 200 Hz.

This method is based on hoop strain measurement using four strain gauges oriented. The strain gauges are equally spaced around the circumference in 90 degrees increments. Longitudinally, two strain gauge stations are placed on a sufficiently long straight pipe section (distant from structural discontinuity estimated by formula $2.5\sqrt{Rt}$, R is defined as (R1 + R2) /2 and t is defined as (t1 + t2) /2 (where t1 and t2 are the minimum thicknesses at each of the regions considered, and R1 and R2 are the minimum midsurface radii of curvature), outside of suspect locations for generation of acoustic pressure waves. The longitudinal spacing is designed to avoid half-wavelengths of the waves. Therefore, the spacing is less then C/2f, where C is the speed of sound of the medium inside the pipe at applicable pressure and temperature and f is the upper bound frequency of 200 Hz.

The strain reading from the strain gauge stations are calibrated for the particular geometry of the pipe section as described in the equation below. The pressure signals occur at a higher frequency than temperature fluctuations, and any possible bending effects due to pipe vibration are eliminated as a result of the strain gauges circuit setup. The strain oscillation reading, for a predetermined period (typically a few seconds), is caused by acoustic pressure waves only and is transformed into pressure amplitudes. This is accomplished by averaging the strain gauge readings, and subtracting the time-averaged mean to obtain the oscillating strains that are related to oscillating pressure. The sampling rate of measurements should be at least 2000 Hz. This strain oscillation will be directly transformed into pressure amplitudes based on the following equation. This equation assumes that the passing wave does not affect the axial stresses.

$$P = \frac{\varepsilon_\theta \times E\left(R_O^{\,2} - R_I^{\,2}\right)}{2R_I^{\,2}}$$

Equation 6:

To account for axial stress impact on hoop stress:

$$\varepsilon_\theta = \frac{\sigma_\theta - \nu\sigma_{Axial}}{E} = \frac{P}{E}\left(\left(\frac{2R_I^{\,2}}{R_O^{\,2} - R_I^{\,2}}\right) - \left(\frac{\nu R_I^{\,2}}{R_O^{\,2} - R_I^{\,2}}\right)\right) = \frac{P}{E}\left(\frac{(2-\nu)R_I^{\,2}}{R_O^{\,2} - R_I^{\,2}}\right)$$

Equation 7:

The pressure is then:

$$P = \left(\frac{(E \times \varepsilon_\theta)\left(R_O^{\,2} - R_I^{\,2}\right)}{(2-\nu)R_I^{\,2}}\right)$$

Equation 8:

Where: ε_{Hoop} is measured strain oscillation amplitude

ε_θ is measured hoop strain oscillation amplitude

E is the Young's modulus of the pipe material

R_O is the pipe outer radius

R_I is the pipe inner radius

P is the calculated pressure

The signal registered by the strain gauges is converted into pressure and its frequency content is computed. To determine magnitudes of interfering waves, a decomposition of the received signal is necessary. A decomposition method developed for two microphones is applied. The attenuation along the pipe is assumed to be negligible due to the relatively short distance between the microphones. Should phase change and consequent energy transfer into a particular location of the steam line be considered for attenuation, the decomposition formulation is appropriately adjusted.

Should the axial flow significantly affect the wave velocity traveling upstream and downstream, this effect is incorporated into the general decomposition formulation below. References 18 and 19 document the decomposition solution. The general solution for wave traveling in both directions inside a duct is given by:

$$P(x) = \left[Ae^{-jkx} + Be^{jkx}\right]$$

Equation 9:

Where: P(x) is total acoustic pressure at position x, A and B are complex magnitudes of the sound wave traveling in positive and negative direction of x respectively

If pressure P at location x is measured and location x (placement of strain gauge) is known, then it requires two strain gauge stations at locations x1 and x2 to generate two equations to solve two unknowns variables A and B, then use Equation 9 for determination of magnitudes of pressure waves at arbitrary location x.

Equation 10:
$$P_{Station1} = \left[Ae^{-jkx_1} + Be^{jkx_1} \right]$$

Equation 11:
$$P_{Station2} = \left[Ae^{-jkx_2} + Be^{jkx_2} \right]$$

Where: $P_{Station1}$ is pressure determined by measure of strain and conversion to pressure at strain station 1

$P_{Station2}$ is pressure determined by measure of strain and conversion to pressure at strain station 2

k is wave number

Alternative method is to directly solve for A and B using following Equations 12 and 13, then use Equation 9 for determination of magnitudes of pressure waves at arbitrary location x.

Equation 12:
$$A = \frac{P_{Station2} - P_{Station1} e^{jk\Delta x}}{e^{-jk\Delta x} - e^{jk\Delta x}}$$

Equation 13:
$$B = -\frac{P_{Station2} - P_{Station1} e^{-jk\Delta x}}{e^{-jk\Delta x} - e^{jk\Delta x}}$$

Where: $P_{Station1}$ is pressure determined by measure of strain and conversion to pressure at strain station 1

$P_{Station2}$ is pressure determined by measure of strain and conversion to pressure at strain station 2

k is wave number

Δx is distance between strain gauges

x is arbitrary location of the wave decomposition

A.2.4 Uncertainties and Bias Associated with the Acoustic Frequency of the Cavity

The uncertainties in the screening criteria provided in Section A.2.1 that are not captured with the correlation for the Strouhal number (Equation 3) are related to the following:

- The acoustic frequency of the cavity.
- The free stream velocity (U) of the flow in the main pipe, or the local velocity at the cavity opening, which may be higher than the free stream velocity to create a different vortex shedding frequency that will excite the acoustic cavity.

- The diameter of the branch (d).

By considering these uncertainties through the variables in the empirical correlation for the Strouhal number, a lower bound value for the Strouhal number is computed to bias comparison to the screening acceptance criteria of 0.63, which verifies that acoustic resonance in the piping systems is avoided during plant operating conditions. The uncertainties in these three characteristics inherent to acoustic resonances are discussed in the following sub-sections.

A.2.4.1 Uncertainties and Bias Associated with the Acoustic Frequency of the Cavity

The first acoustic frequency ($f_{acoustic}$) of the depth or organ mode for a deep cavity with a narrow opening is defined by the relation:

$$f_{acoustic} = \frac{C}{4L}$$ Equation 2 with N=1

This relationship shows that the acoustic frequency of the cavity is proportional to the speed of sound (C). The speed of sound is a function of the temperature, pressure, and quality of the pipe flow. Uncertainties in the plant measurement of the temperature and pressure in the piping system could lead to inaccurate values for the density of the fluid and give a different velocity for the speed of sound in the piping system. Considering the operating pressure and the design temperature of the piping system, as opposed to the ambient plant operating conditions, a lower bound value for the speed of sound is obtained to eliminate uncertainties associated with the speed of sound. This will bias the Strouhal number computation for comparison to the screening criteria, which will verify that acoustic resonance in the piping systems will be avoided during plant operating conditions.

Although the expression for the acoustic frequency defines the physical depth of the cavity (L), the acoustic mode will attenuate into the main pipe, which creates a characteristic depth (L_{eff}) of the cavity. The acoustic frequency of the cavity and the Strouhal number can be conservatively determined by considering the effective depth of the cavity through the following relationship:

Equation 15: $$L_{eff} = L + 0.3(d)$$

where,

"d" is the diameter of the opening of the cavity.

If the design of the standoff pipe and branch lines, safety relief valves, or any other component attached to a piping system create an acoustic cavity that can not be characterized as a narrow deep cavity in the piping system, the characteristic length of the unique acoustic cavity will be determined with other empirical relations. This verifies that the most representative value is considered to bias the computation of the Strouhal number for comparison to the screening

criteria to provide additional verification that the acoustic resonance in the piping systems will be avoided during plant operating conditions.

A.2.4.2 Uncertainties and Bias Associated with the Free Stream Velocity

Regarding the uncertainties in the free stream velocity (U), there are several factors that could create a local velocity at the opening of the acoustic cavity that would be higher than the free stream velocity in the main pipe. The elbows in the pipe accelerate the flow along the outer radius of the pipe internal diameter (ID). If an acoustic cavity is located downstream and is in close proximity to the elbow, the local velocity of the flow over the opening of the cavity is higher than the free stream velocity in the main pipe, which creates a higher vortex shedding frequency than predicted using the free stream velocity. The variation in the dimension of the pipe ID (or the cross-sectional flow area of the pipe) can create local variations in the flow velocity. The uncertainty in the measurement of the mass flow rate by the plant instrumentation also influences the magnitude of the effective velocity. The uncertainty in the velocity as a function of the mass flow rate is exacerbated by the uncertainty in the fluid density as a function of the temperature and pressure of the flow measured by the plant.

These uncertainties in the local velocity near the opening of the acoustic cavity will be accounted for by considering a 10 percent increase in the mass flow rate for full power, normal operating conditions, and transient conditions, to provide an upper bound effective velocity for which the Strouhal number will be determined and then compared to the screening criteria for acceptance (S = 0.63). By adjusting the mass flow rate, the uncertainties associated with the local velocity at the opening of the cavity are eliminated to bias the computation of the Strouhal number for comparison to the screening criteria to provide additional verification that acoustic resonance in the piping systems will be avoided during plant operating conditions.

A.2.4.3 Uncertainties and Bias Associated with the Branch Opening Diameter

The frequency of the vortices generated by the discontinuity of branch opening is proportional to the free stream velocity (U) and inversely proportional to its diameter (d) and is empirically determined through the relationship:

Equation 16: $$f_{vortex-shedding} = \frac{SU}{d}$$

The uncertainties of the free stream velocity in the computation for the vortex shedding frequencies is addressed in Section A.2.4.2. Regarding the branch diameter (d) and the uncertainties associated with the vortex shedding frequencies, Section A.2.1 describes the influence of the blend radius ("r") of the mouth of the branch opening on the computations for the Strouhal number through Equation 5, which is the following:

Equation 17: $$f_{vortex-shedding} = \frac{SU}{(d+r)}$$

The consideration of a characteristic diameter ($d_{eff} = d + r$) to determine the vortex shedding frequencies, which are equated with the acoustic frequency of the cavity, is developed in the screening criteria for acoustic resonance by comparing the Strouhal number to 0.63. The resulting computation for the Strouhal number is biased to address uncertainties of the parameters that impact the vortex shedding frequency of the cavity.

A.3 Vibration Measurement Instrumentation

The low end of the natural frequency range is the most important, as the highest frequency of loading is not more than approximately a few hundred Hertz, which is below the high end of the range of instrumentation. The lowest natural frequency computed for most piping systems is at the low end of the frequency range specified.

The typically lower frequency limit associated with accelerometers mounted to an object compared to hand-held vibration instruments held up against an object will be considered in the choice of vibration instruments for the particular application.

A.3.1 Choice of Locations for Vibration Instrumentation

The primary method used for vibration acceptance criteria described in this appendix follows the guidance of Reference 12, vibration monitoring group 2 (VMG 2). One of the assumptions inherent to this method is that the maximum piping vibration is measured. Therefore, experienced engineering personnel will be involved in determining the locations of maximum piping vibration, considering the piping routing, support locations, and accessibility. Preliminary locations selected for measurement of the reactor coolant system, main feedwater and main steam system piping are shown in Figures A-2 and A-3. In the event that accessibility precludes measurement of a location of maximum piping response, measurements will be taken where accessible and conservative acceptance criteria will be used for vibration measurements at these locations.

A.4 Acceptance Criteria

Reference 12 is used as the basis for the acceptance criteria for the vibration of piping. VMG 2 is used as the primary method of determining acceptability of vibration. In this method, the vibration velocities are compared to acceptable values, which are determined by beam analysis for the boundary conditions and basic shape of a piping routing. Typical values for use in determining acceptance criteria are provided in Reference 12.

Reference 12 assumes that the vibration is a pure-tone sinusoid at the first natural frequency of the piping. A correction factor is described in Reference 12 to account for vibration at a frequency different from that of the first mode.

Piping vibration is typically more random than the assumed pure-tone sinusoid assumed in Reference 12, and the guidance provided in References 2 and 4 accounts for this, as a clarification of the method described in Reference 12. The RMS of the vibration amplitude is

computed from measurements, and consideration of the range of values of vibration is used to provide a multiplier on the RMS. This value is then compared to the acceptance criterion of the limiting velocity that is developed according to Reference 12.

Because the assumption is made in Reference 12 that the vibration occurs at the first mode of the piping, the measured frequencies are compared to those of the first mode computed, when such computations are performed, and the appropriate correction factor to the acceptance criterion is applied as described in Reference 12.

For small-bore piping that is inaccessible, vibration monitoring group 3 (VMG 3) may be used, which involves visual observation by experienced personnel to determine acceptability of piping vibration.

Figure A-1—Shear Wave Acoustic Resonance

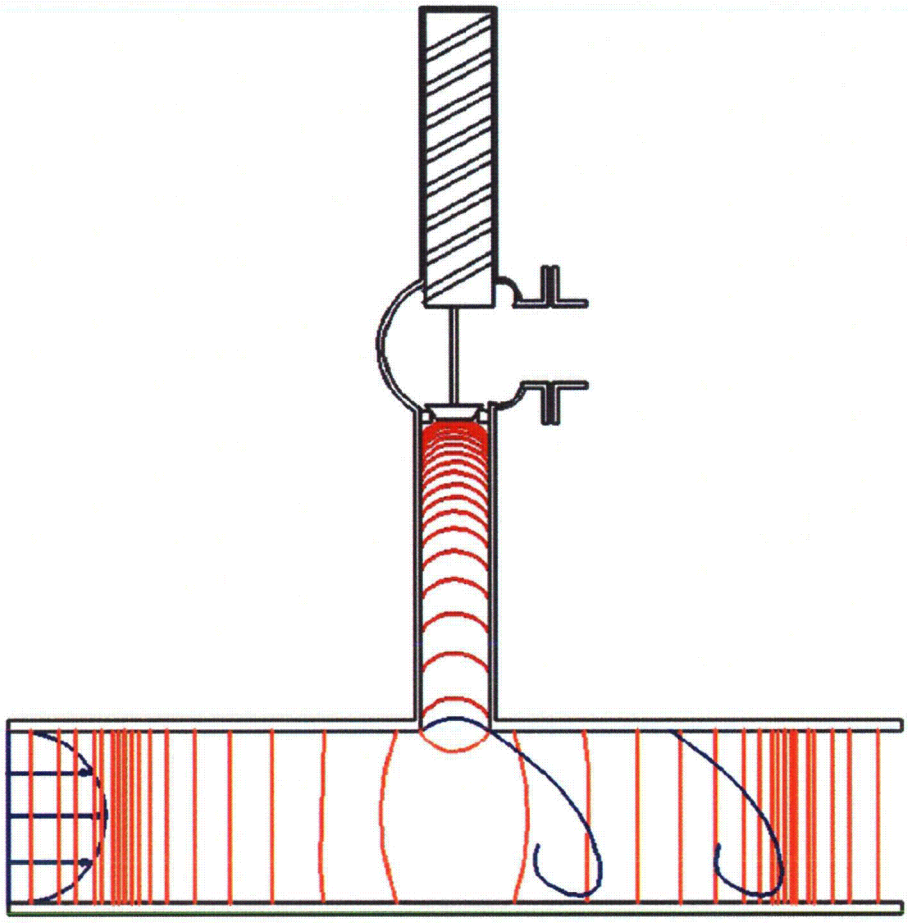

Figure A-2—Positions of VMS Transducers in the MSL and the MFWL

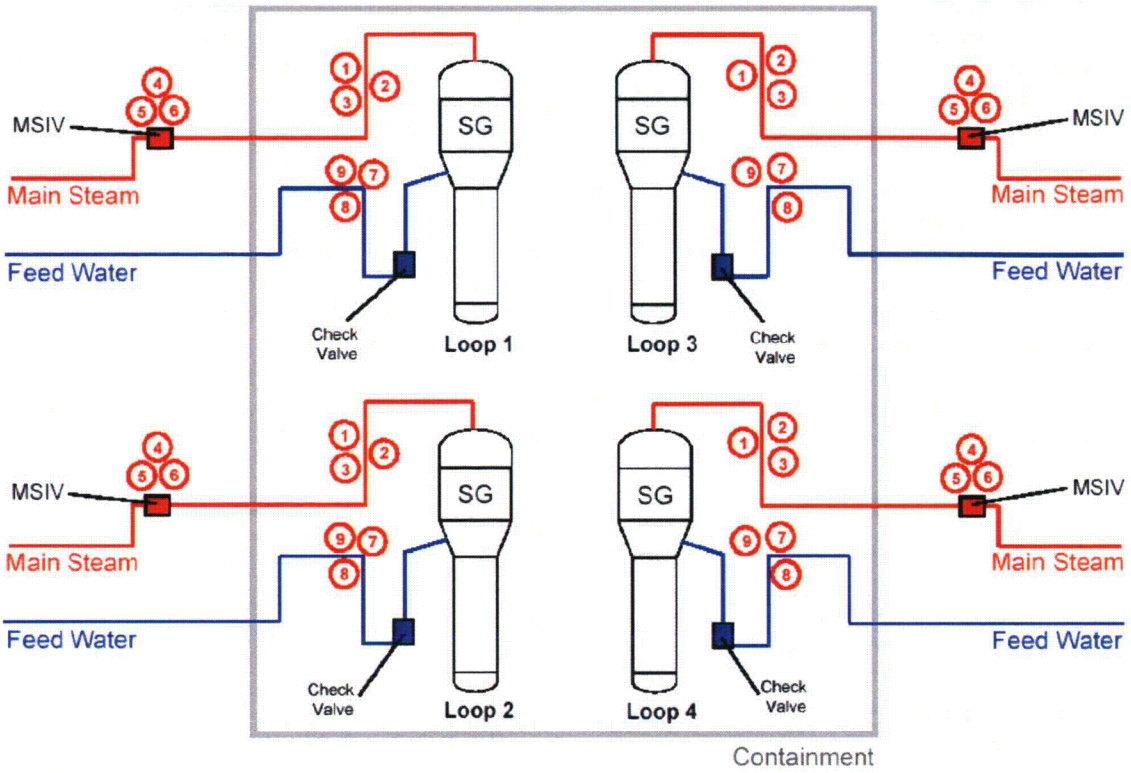

Figure A-3—Positions of VMS Transducers in the Reactor Coolant System

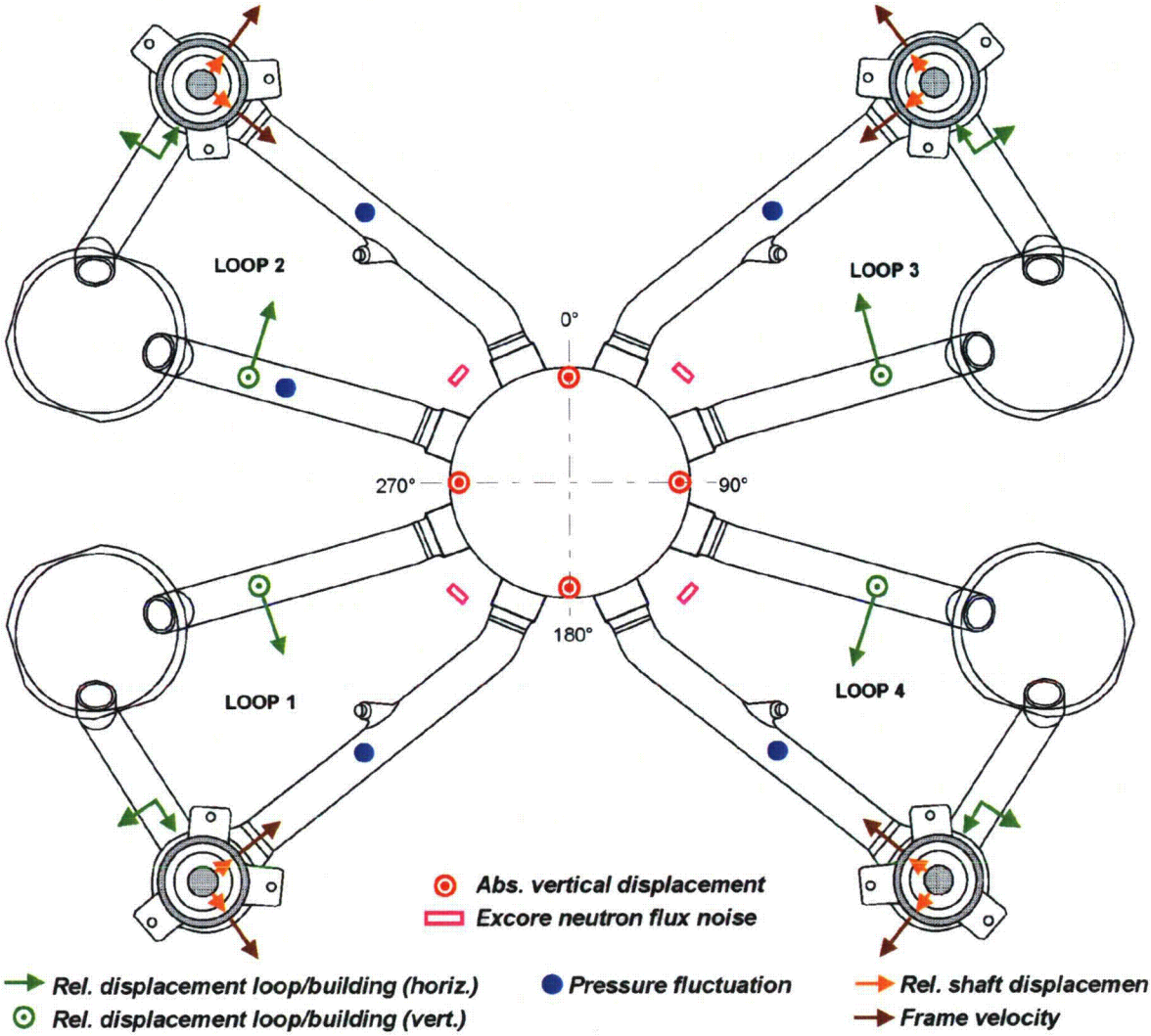

APPENDIX B: VIBRATION ASSESSMENT OF THE RSG UPPER INTERNALS

B.1 Scope

This appendix provides a summary of the FIV evaluations performed for the U.S. EPR RSG upper internals and also reviews the operating experience of similar RSG upper internal designs to assert the integrity of these components. This appendix also provides the engineering justification for the exception taken with Reference 1 for the RSG upper internals.

The U.S. EPR RSG upper internals are classified a prototype design by the definitions provided in Reference 1.

B.2 Operating Experience with RSG Upper Internal Design Similar to the U.S. EPR

The U.S. EPR RSG is the 79/19TE design. The following nuclear plants are currently operating in Europe with the 73/19TE and the 79/19T RSG design, which has upper internals that are similar to the U.S. EPR RSG. To date, no flow-induced vibration problems related to the steam generator upper internals have occurred at these plants:

- 79/19T RSGs of the Doel Unit 4 (SG replacement occurred in 1996).
- 79/19T RSGs of the Tihange Unit 3 (SG replacement occurred in 1998).
- 73/19TE RSGs of CZB1 (SG replacement occurred in 1996).
- 73/19TE RSGs of CV2 (SG replacement occurred in 1999).

In part, the justification of the integrity of the U.S. EPR RSG upper internals regarding flow induced vibration is assessed based upon these operating plants. The distinction of "E" in the identification of the model design between the U.S. EPR and the Belgian plants refers to the addition of the axial economizer in the tube bundle, which is used to improve the thermal efficiency of the design over the 79/19T RSG design.

B.2.1 Comparison of RSG Upper Internal Designs

The U.S. EPR RSG upper internals consists of two primary components: the [ ] two stage primary steam separators (cyclone, type S 335-2) and the steam dryers (STAR type). In the upper part of the tube bundle, the steam flow exiting the u-bend is ducted to the [ ] high-efficiency separators with piping between the roof of the tube bundle wrapper and the entrance to the steam separators (See Figure B-1). The primary steam separators are a cyclonic design in which two swirl vanes create centrifugal forces to separate the steam and liquid mixture (See Figure B-2). The liquid is re-circulated to the tube bundle and the steam exits the separators and enters the [ ] dryer cells arranged vertically in a STAR pattern. Each dryer cell is primarily constructed of chevron-type dryer vanes which create directional changes in the vapor to further

separate the steam/water mixture. [ ] cells are arranged around the periphery, and the other [ ] are located in a radial direction (See Figure B-3).

There are two operating plants that utilize the 79/19T RSG design. Comparisons of the thermal hydraulic conditions and other design aspects of the steam separators and dryer are provided in Table B-1. This table shows that the secondary side mass flow rates and the densities entering the steam drum are approximately the same for these plants. The steam dryer design (STAR) of the operating plants is identical to the U.S. EPR steam dryer design in terms of material specification, geometry, and support configuration. The replacement steam generators at Doel and Tihange were placed in service between the years of 1996 and 1999. There is significant operating experience with the STAR steam dryer design.

However, the two-stage primary steam separators for the U.S. EPR are a first of a kind and no operational experience exists for this component. For this reason, FIV analysis of the primary steam separators is performed to justify the integrity of this component.

Table B-1—Comparison of RSG Upper Internals between the U.S. EPR and Other Plants Currently Operating

Figure B-1—U.S. EPR RSG Upper Internals

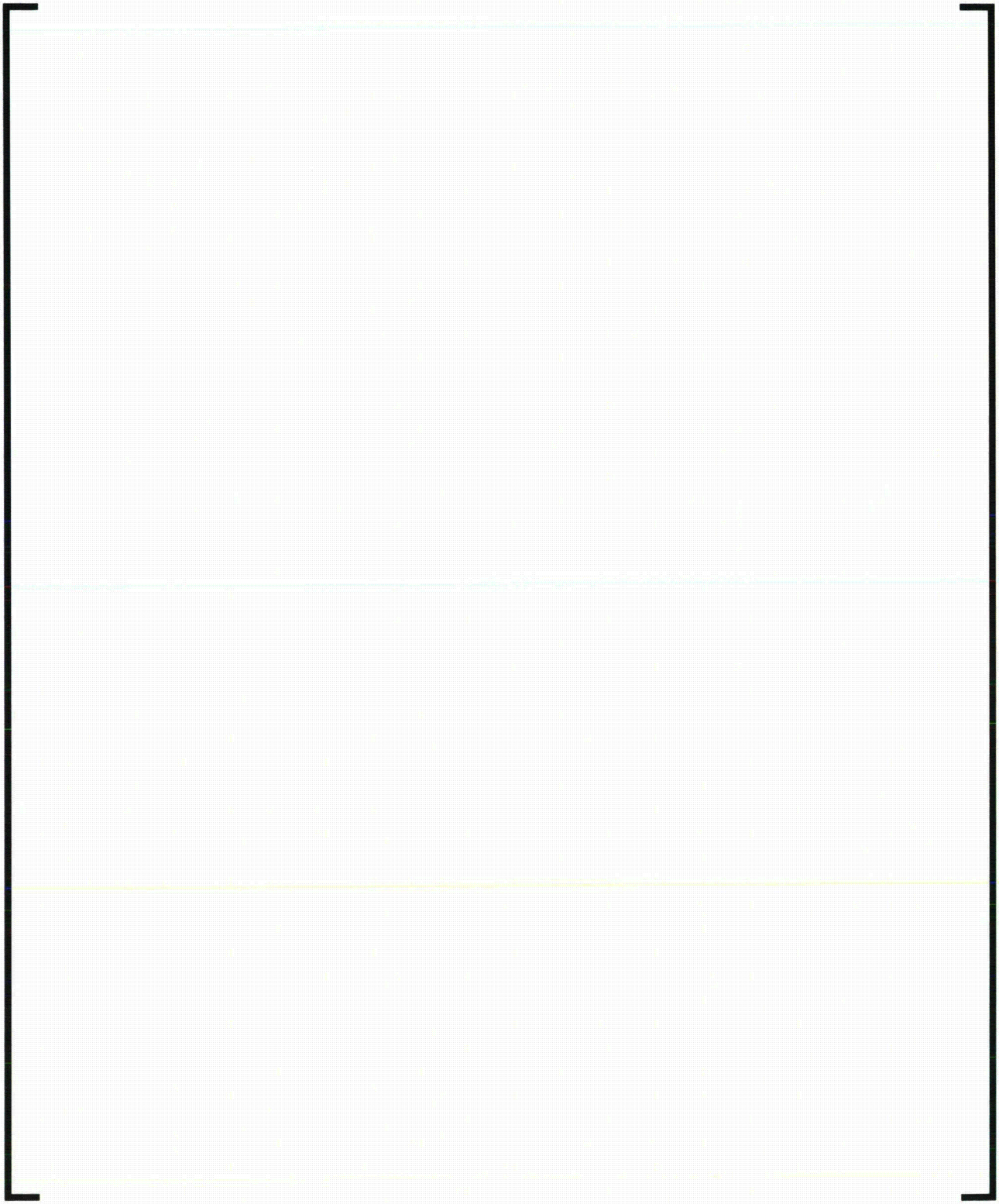

Figure B-2—U.S. EPR RSG Two Stage Primary Steam Separators (Type S 335-2)

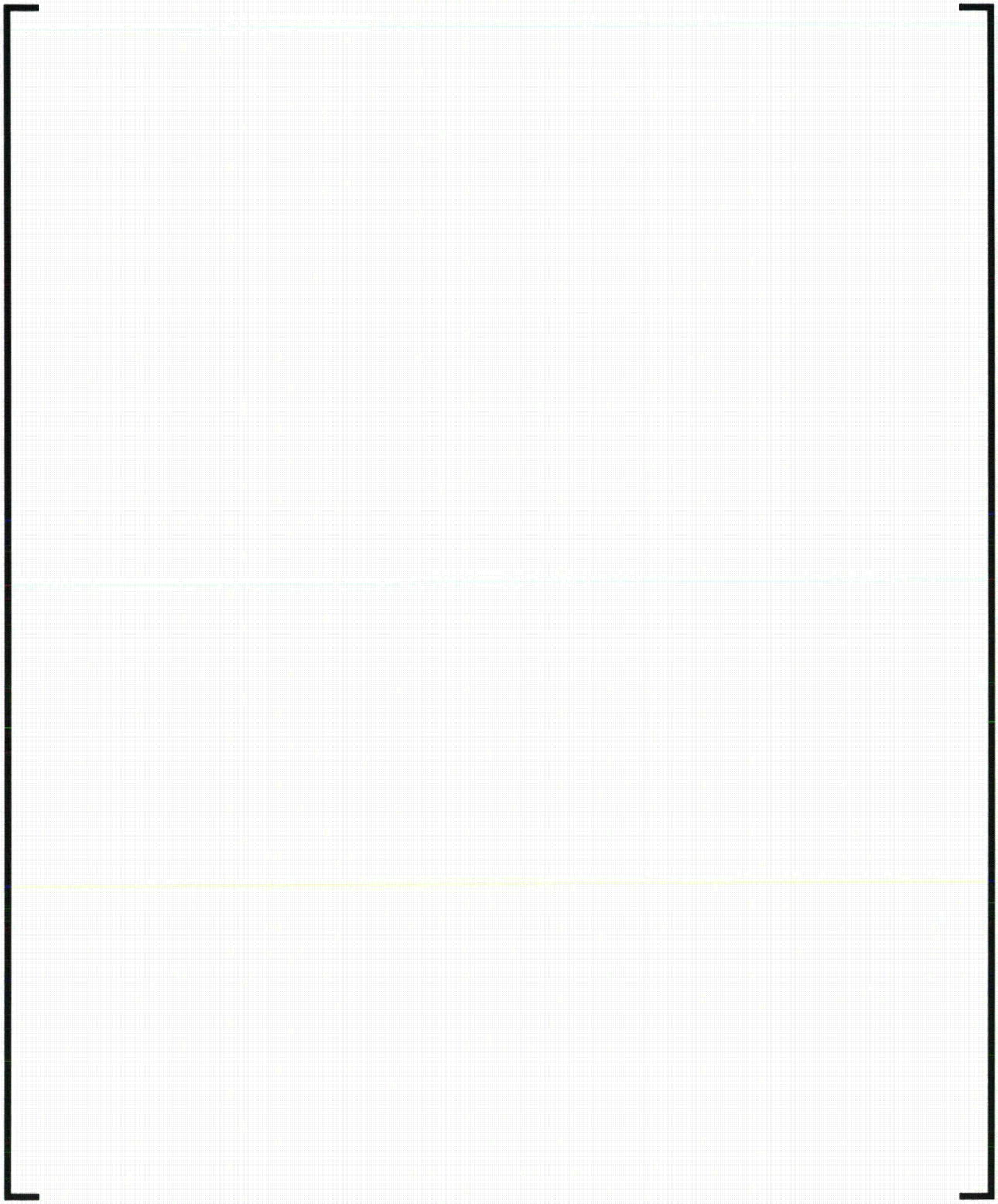

Figure B-3—U.S. EPR RSG Steam Dryers

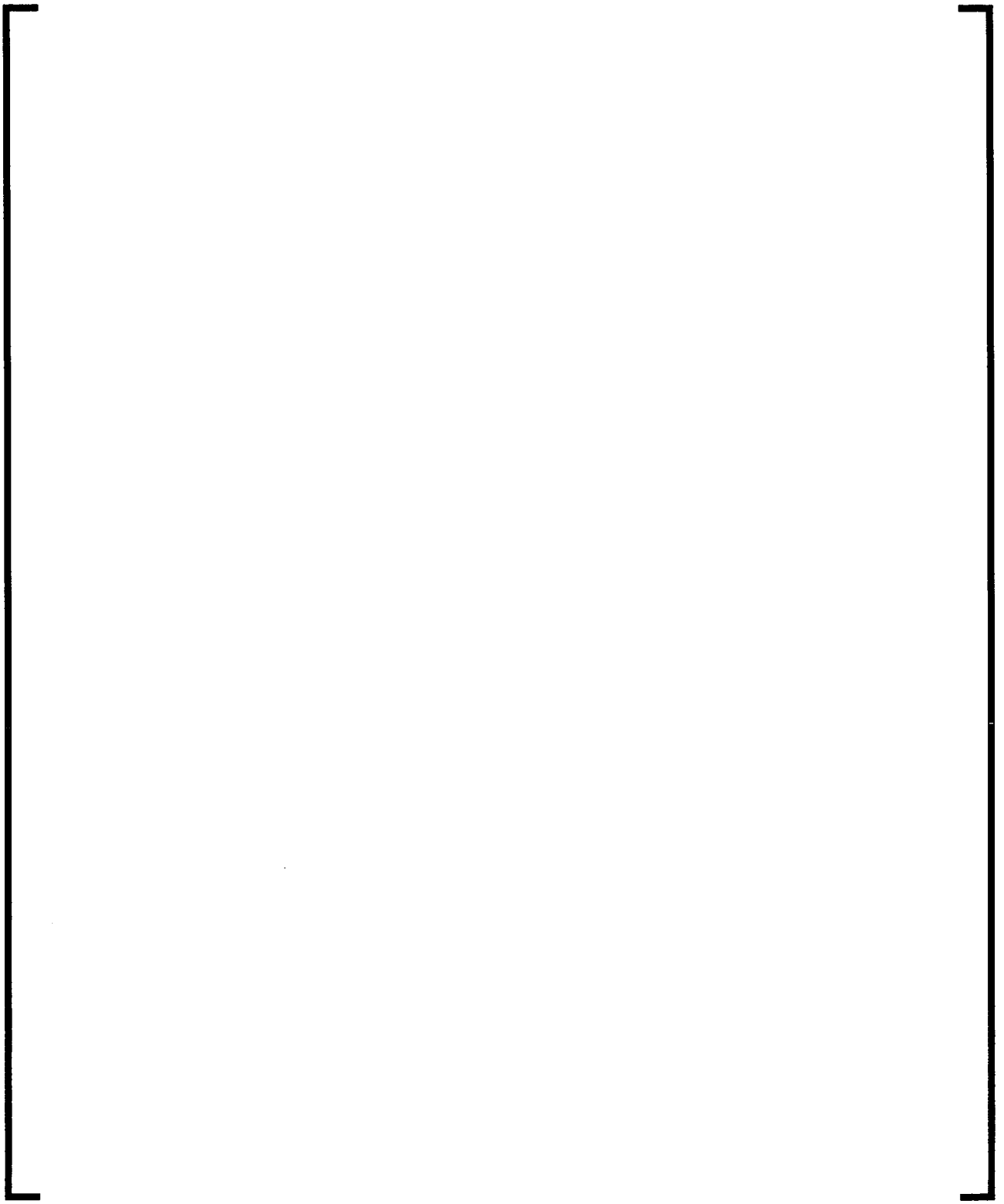

B.3 FIV Evaluation of the Primary Steam Separators

As shown in Table B-1, there are no operating RSG designs in Europe or the U.S. that employ the type S 335-2 two stage primary steam separators. Therefore, the integrity of the primary steam separators is demonstrated through the analytical evaluations described in Section B.3.1 through Section B.3.3 for flow excitation due to random turbulence, acoustic resonance, and axial leakage flow. Section B.3.4 describes the influence of the FIV inputs and the associated conservatisms to demonstrate that the primary steam separators are not susceptible to significant flow-induced vibrations. Therefore, instrumentation of the primary steam separators during hot functional testing to determine the actual FIV inputs and to confirm the amplitudes of vibration of this component is not necessary and the exceptions to the guidelines of Reference 1 are justified for the primary steam separators.

B.3.1 Random Turbulence due to Parallel Flow Excitation

The analytical methodology implemented for the full scale evaluation of the primary steam separators is identical to that performed for the FDD in Section 4.3.2.1. However, there are unique differences in the design inputs for the primary steam separators which are described in this section.

The FEM of the primary steam separator and the entrance pipe to the separator is created with 3-D beam elements using the CASS program to obtain the natural frequencies and the associated mode shapes with a cutoff frequency of approximately 350 Hz. The total linear mass density of the separator is determined considering the hydrodynamic mass density that the separator displaces through the following relation:

$M_t = (A_i)(\rho_{fluid}) + (A_o)(\rho_{fluid}) + (A_t)(\rho_{metal})$ linear mass density of separator.

$\rho_{eff} = M_t / A_t$ effective density of separator.

The product, $(A_o)(\rho_{fluid})$, is the hydrodynamic linear mass density that the separator displaces (considering an added mass coefficient of 1.0). The product, $(A_t)(\rho_{metal})$, is the linear mass density of the separator; and the product, $(A_i)(\rho_{fluid})$, is the linear mass density of the fluid contained in the separator. The modal frequencies of the pipe-separator assembly are provided in Figure B-4.

The excitation of these frequencies and eigenvectors resulting from the turbulent parallel flow through the pipe-separator assembly is based upon the finite element implementation of the acceptance integral method, which has been outlined in Section 4.3.2.1, using the computer program "PCRANDOM." The unique FIV inputs for the primary steam separator are as follows:

Thermal Hydraulic Conditions

A nominal free stream axial velocity of [ ] inch/sec through the steam separator consistent with full power, steady state, normal operating conditions is evaluated.

Structural Damping

The total damping coefficient is a composite of the following damping mechanisms:

- The structural damping associated with the hysteresis of the material.
- The structural damping created by the non-linear interactions of the lateral supports of the steam separator.
- The hydrodynamic damping of steam mixture.

A conservative viscous damping ratio of [ ] is applied to the pipe-separator assembly. The uniform structural damping coefficient is set to two times the viscous damping coefficient to achieve an equivalent viscous damping at resonance.

Correlation Length and Convective Velocity

For extremely turbulent flow conditions in confined channels, the correlation length (λ) of the forcing function acting along the length of the pipe-separator assembly is equal to approximately 40 percent of the hydraulic radius (Reference 4, Equation 8.65). For extremely turbulent flow conditions in confined channels, the convective velocity is approximately equal to 100 percent of the axial flow velocity (Reference 4, Equation 8.58).

Pressure PSD

The pressure PSD that is applied to the pipe-separator assembly is measured from turbulent flow testing (without cavitation) in extremely turbulent single phase flows in confined channels where there are no well-defined boundary layers, such as those encountered in industrial piping systems with elbow, valves, and changes in cross sections. The pressure PSD is taken from Reference 4, Equation 8.70 and graphically presented in Figure B-6. The upper bound curve shown in this figure is used for the evaluation performed for the piping-separator assembly. Figure B-9 provides the dimensional pressure PSD for a frequency range of 0 to 250 Hz, which bounds the frequencies that are evaluated in the analysis of the steam separators.

The structural model for the steam separators evaluates the nominal (design) dimensions of the components to determine the natural frequencies and mode shapes of these components. As such, the analytical model does not specifically consider the manufactured tolerances associated with the geometry of the structures and the differences in material properties values established in the ASME code and the as-built values. The rationale used to disposition the bias and uncertainty of the modal frequencies of the RPV lower internal assembly described in Section 4.2.7.1.3 is identical for the steam separators. Since the fluid-structure coupling mechanism for random turbulence is weak, the slight variation in the natural frequencies attributed to manufactured tolerances and variation of the material properties do not significantly alter the forcing function and the response of the steam separators. The uncertainty in the response of the separators associated with these tolerances in the natural frequencies is estimated to be less than $\pm$ 5 percent of the amplitude of vibration.

Figure B-4—Pipe-Separator Frequencies and Mode Shapes (In-Plane X-Y Plots)

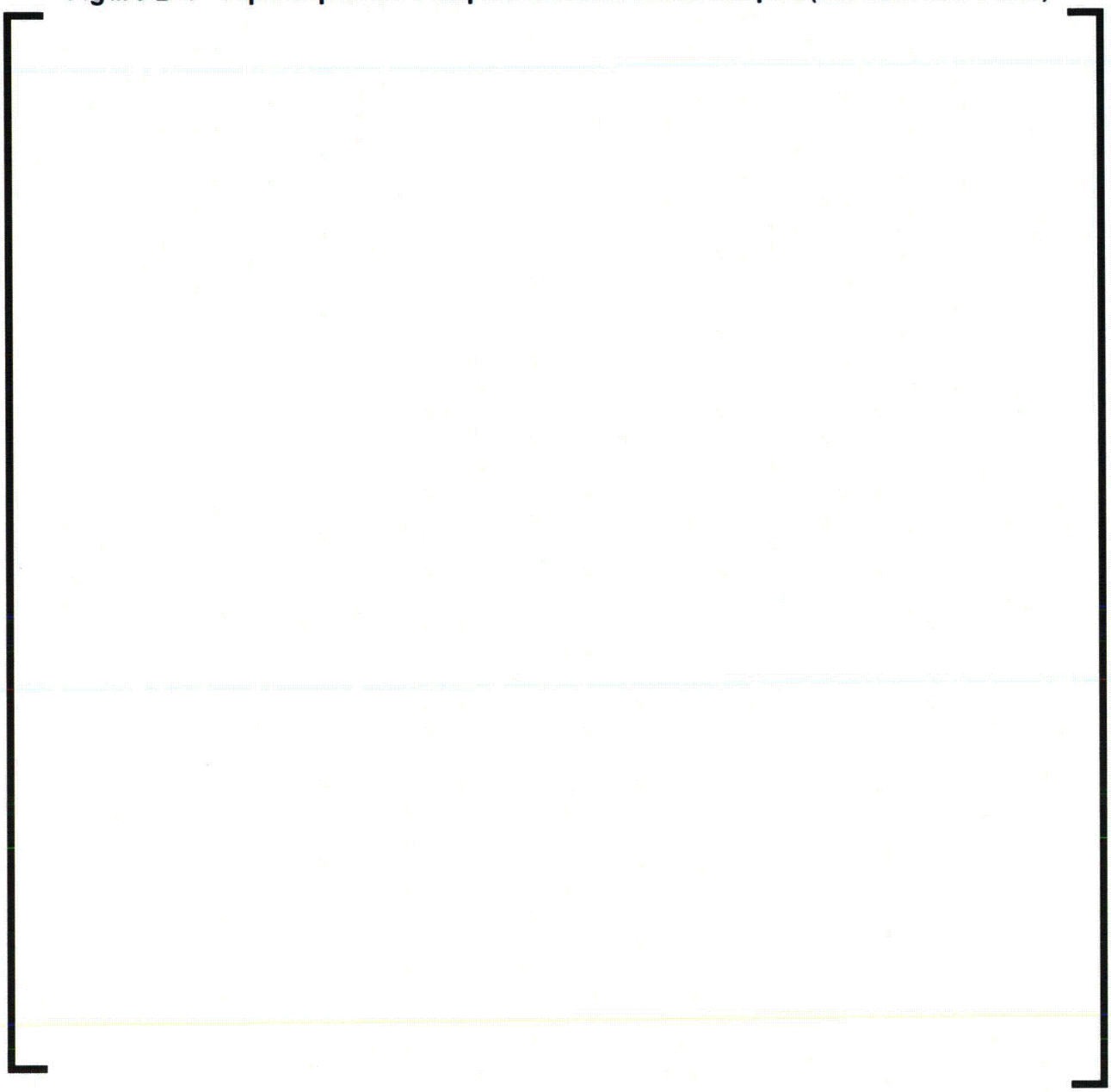

Figure B-5—Pipe-Separator Frequencies and Mode Shapes (Out-of-Plane Z-Y Plots)

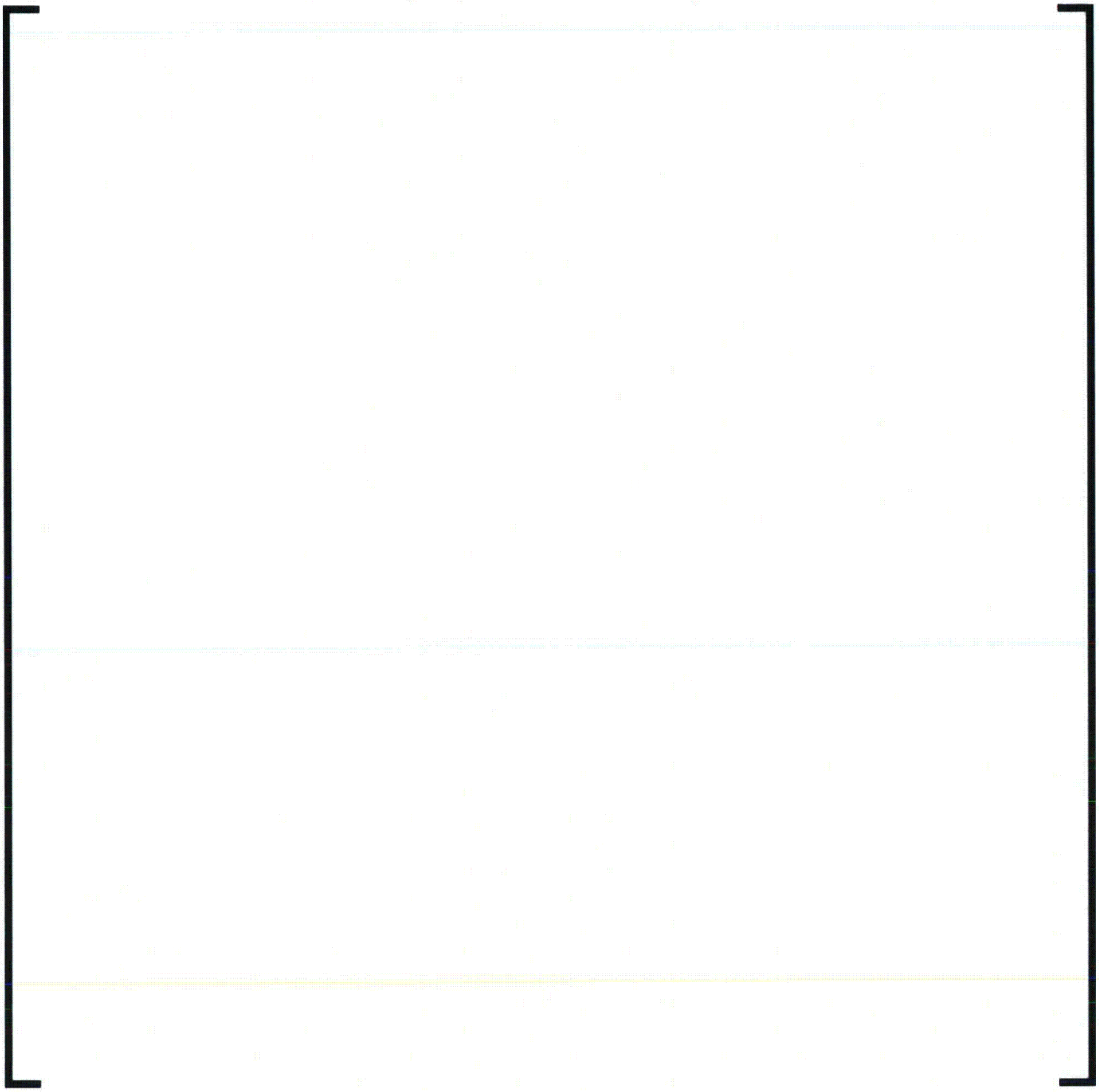

Figure B-6—Single Sided Non-Dimensional PSD for Confined Annular Flow

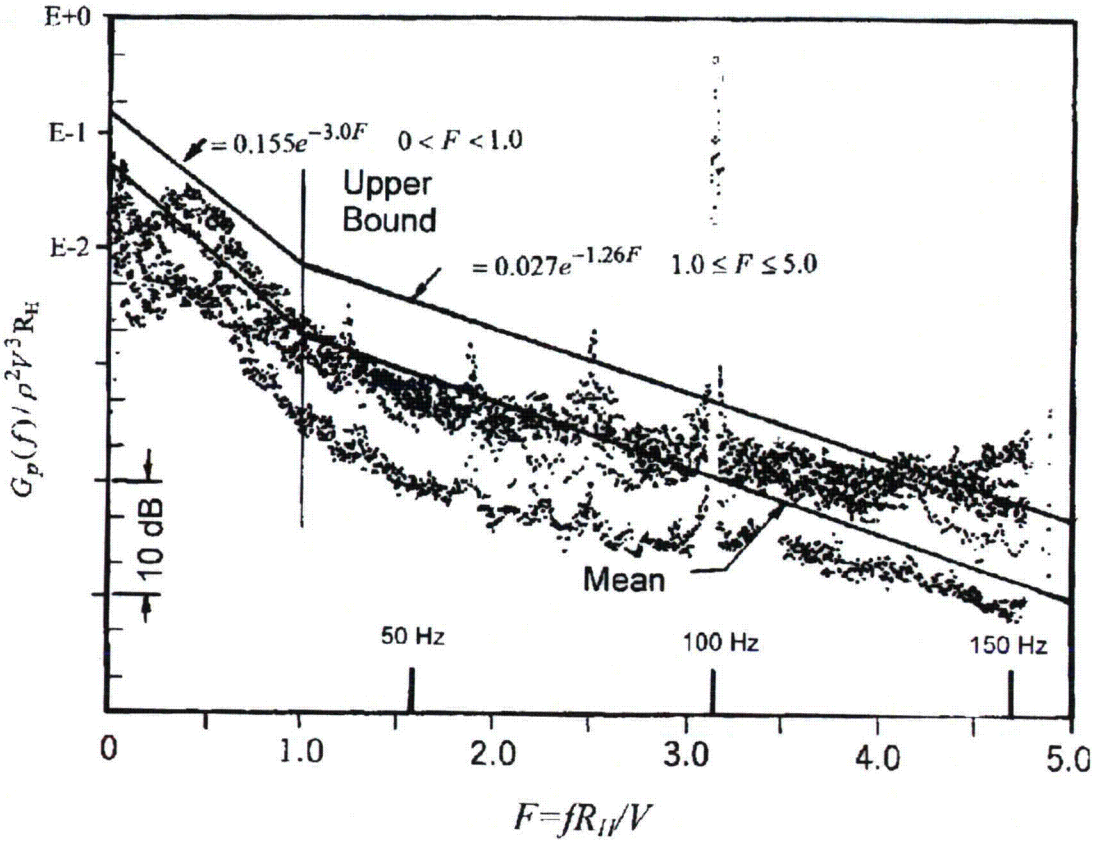

$$\frac{G_p(f)}{\rho^2 V^3 R_H} = 0.155e^{-3.0F} \text{ for } 0 < F < 1.0$$

$$= 0.027e^{-1.26F} \text{ for } 1.0 \le F \le 5.0$$

Where

$$F = \frac{f R_H}{V}$$

Notes for Figure B-6:

1. Per Reference 4, Figure 8.17.

B.3.2 FIV Acceptance Criteria

B.3.2.1 Acceptance Criteria for Displacements

The acceptance criterion for displacements due to turbulence-induced vibration is based on one-half the gap clearance between adjacent separators. Because the clearance between the entrance pipes is smaller than the clearance between the separators, the minimum acceptable displacement is conservatively based upon the clearance between the entrance pipes. The nominal pitch between the entrance piping is approximately [ ] inches and the nominal pipe OD is approximately [ ] inch. One-half of the gap clearance is:

C_{min} = (Pitch – OD) /2 = [ ] inch

Because the computed displacement response (inch, rms) to turbulence is based on a probability of excursions, C_{min} as calculated above, it is divided by a factor of 5 or 5 sigma, which is representative of approximately a 100 percent probability that this allowable displacement will not be exceeded. The acceptable displacement for vibration induced by flow turbulence is [ ] inch, rms.

B.3.2.2 Acceptance Criteria for Fatigue

The criterion established in Section 4.2.6.2 using fatigue curve "C" is applied to the primary steam separator. An allowable stress of [ ], at 10^{13} cycles is conservatively used and neglects corrections to this value resulting from the difference in the elastic modulus between the fatigue curve and the pipe-separator assembly.

An FSRF of 1.0 is applied at cross sections that are removed from any structural discontinuity. An FSRF of 4.0 is conservatively applied at cross sections of local structural discontinuities, particularly the geometrical transitions, of the primary separator piping to conservatively accounts for their stress amplification effects.

B.3.3 Response of the Pipe-Separator Assembly to Random Turbulence

B.3.3.1 Displacement RPSD for the Pipe-Separator

The linear-log scale plots for the in-plane and the out-of-plane dimensional response PSDs of the pipe-separator assembly are shown respectively in Figure B-7 and Figure B-8. These figures predict the response for the first seven natural frequencies of the pipe-separator assembly considering a cut-off frequency of 350 Hz. Note that mode 4 (~ [ ] Hz) is an axial mode of the structure and does not create a translational response. As expected, the majority of the response occurs from the fundamental frequency (beam mode, [ ] Hz).

Table B-2 and B-3 report the RMS displacement and stress in the pipe-separator assembly resulting from the turbulent excitation of the parallel flow along the length of this structure. A

maximum stress of [ ] psi, rms at a zero crossing frequency of [ ] Hz occurs at the base of the pipe-separator assembly (node 1) in the in-plane direction. Both the maximum stress and displacement response are below the acceptable FIV limits defined in Section B.3.2.

Table B-2—Pipe-Separator Displacements (RMS Response)

Table B-3—Pipe-Separator Stress (RMS Response)

Note(s) for Table B-3:

1. The stresses reported in this table do not include the stress amplification effects of the structural discontinuities of the primary separator. Applying a conservative value of 4.0 for the FSRF, a maximum alternating stress of [ ] is obtained, which is much less than the allowable stress at [ ] at 10^{13} cycles.

Figure B-7—Pipe-Separator In-Plane Displacement Response PSD

Notes for Figure B-2:

1. The node locations shown in this figure are along the length of the pipe-separator assembly with Node 1 at its base (Elev = 0.0 inch) and Node 90 at the top (Elev = [ ] inch).

Figure B-8—Pipe-Separator Out-of-Plane Displacement Response PSD

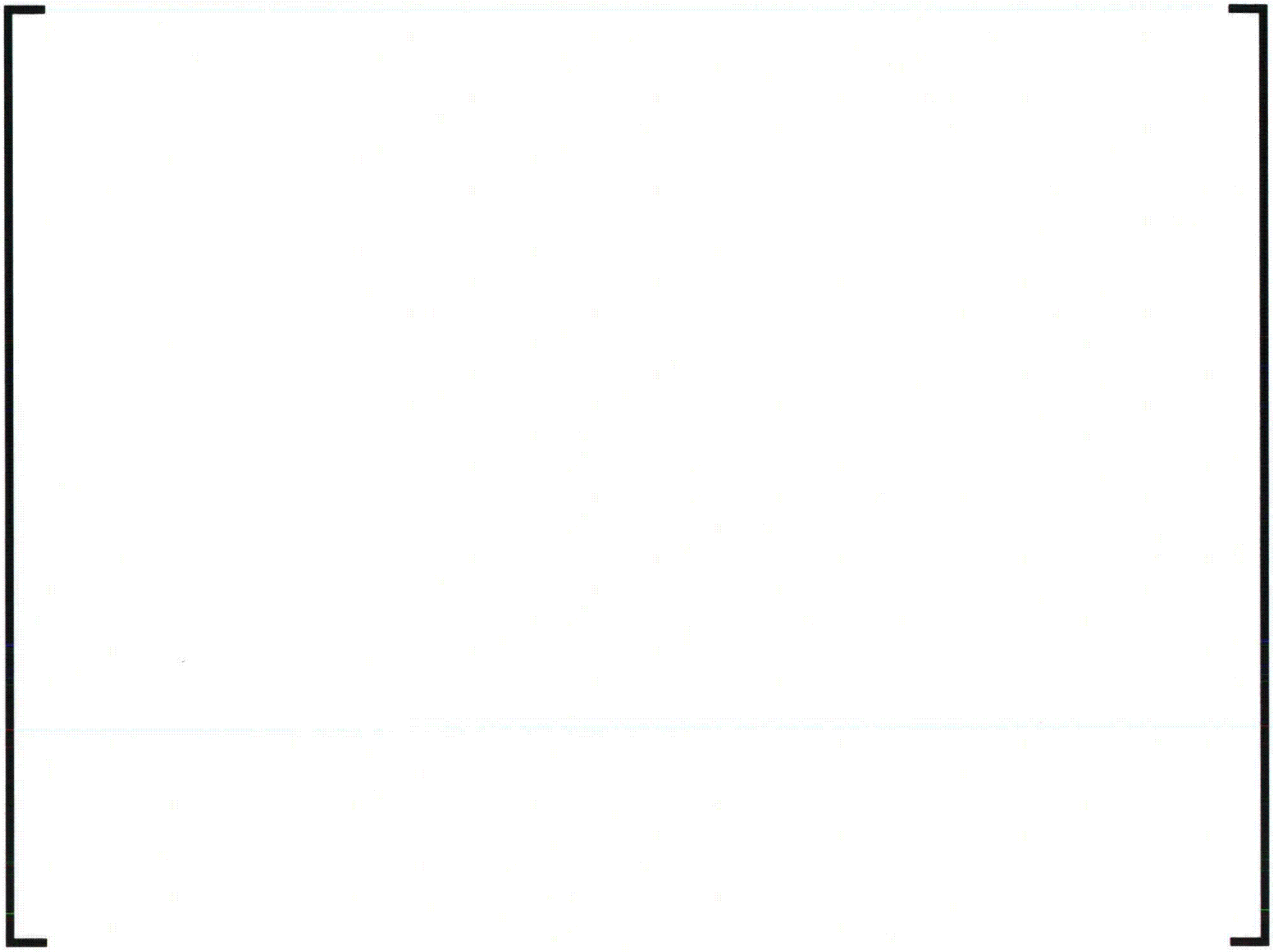

Notes for Figure B-8:

1. The node locations shown in this figure are along the length of the pipe-separator assembly with Node 1 at its base (Elev = 0.0 inch) and Node 90 at the top (Elev = [ ] inch).

Figure B-9—Pressure PSD for Pipe-Separator Assembly

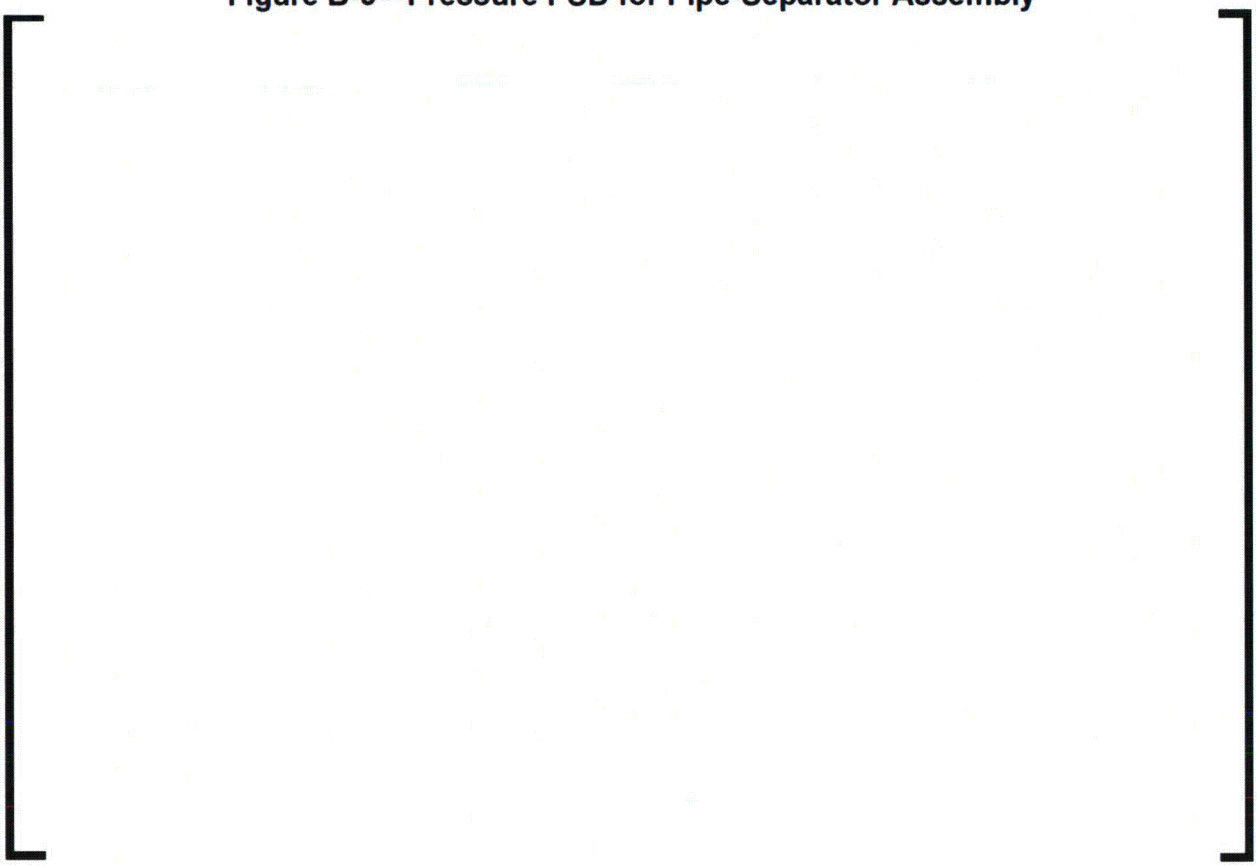

Notes for Figure B-9:

1. The dimensional pressure PSD in this figure is developed from the dimensionless PSD identified with Figure B-6, with a dimensionless frequency range is F=0 to F=5 (or approximately 170 Hz). The range of frequency depicted in this figure (0 to 250 Hz) corresponds to the dimensionless frequency range of F=0 to 7.4. The dimensional PSD in this figure is extrapolated to 250 Hz considering the same slope or decay of turbulent energy between F=1 and F=5, as shown in Figure B-6.

B.3.3.2 Evaluation of Other FIV Mechanisms

Axial Leakage Flow-Induced Vibrations

In the presence of a narrow flow channel surrounded by flexible structures, axial leakage flow-induced vibrations or instability can become a source of excitation. The steam separators have very open flow channels that allow steam to flow unrestricted through these components. This source of excitation is not expected for the primary steam separators.

Random Turbulence Excitation of the Pipe-Separator Due to Cross Flow

The steam separators are not susceptible to flow-induced vibrations created from the turbulence of the secondary side flow conditions that would act upon the OD surfaces of the steam separators. Because the majority of the steam flow is through the steam separator, it is only the recirculation flow created by the steam separators and the steam dryers that have the capability of creating secondary side flow conditions to induce a response. The magnitude of this flow is less than 5 percent of the secondary side flow conditions. Therefore, these structures are not susceptible to turbulent excitation resulting from the cross flow conditions in this region of the upper internals.

Acoustic Resonance Excitation of Primary Steam Separators

It is not expected that the primary steam separators will be susceptible to acoustic excitation created in the main steam or the feedwater piping systems as either the stream dryers or the tube bundle will have disrupted these acoustic pressure waves prior to reaching the separators. However, screening for the conditions that would lead to acoustic resonances in these piping systems will be performed. See Section A.2.1 for the screening methodology that will be implemented to verify that the design of these piping systems is not conducive to creating this source of excitation.

B.3.4 Justification for the Exception to RG 1.20 for the Primary Steam Separators

This section provides the justification that the instrumentation, the acquisition of test data during HFT, and the subsequent interpretation of this data as specified by Reference 1 is not critical when demonstrating the FIV integrity of the U.S. EPR RSG primary steam separators. The justification for this exception, as well as the FIV inputs that are assumed for the FIV analysis of the primary steam separators, is demonstrated in this section.

The three parameters which characterize the relationship between the vibration of the pipe-separator assembly and the turbulent forcing function are the convective velocity, the correlation length, and the PSD function. The degree of coherence between the forcing function and the structural mode shapes is based on the correlation length and the phase relationship of the forcing function between two different points along the length of the piping. The power spectral density function represents the energy distribution of the turbulence in the flow stream as a function of the frequency.

The degree of coherence between the forcing function and the structural mode shapes can be expressed in the following functional form:

$$\Gamma(x',x'',f) = e^{-\frac{|x'-x''|}{\lambda}} * e^{\frac{-i\,2\pi\,f(x'-x'')}{U_c}}$$

The coherence of the forcing function (Γ) between two points along the length of the structure (x' and x'') is dependant on both the correlation length (λ) and the convective velocity (U_c). These two constituents and their compatibility with the mode shapes and frequencies define the degree of coherence between the forcing function and the structure or the joint acceptance. The conservatism of these three FIV inputs and the justification for the exception to the guidelines of Reference 1 is addressed.

Convective Velocity

As stated in Section B.3.3, the majority of the turbulent response of the steam separator is created from the fundamental modal frequency. The parallel flow excitation of the fundamental mode is maximized if the phase relationship between this mode and the convective velocity (U_c) becomes coincident, increasing the coherence of the forcing function. The convective velocity required to create this coincidence with the first modal frequency (Freq = [ ] Hz, cantilever mode shape) is [ ] inch/sec. A convective velocity of [ ] inch/sec (or 100 percent of the mean free stream velocity) is considered in the FIV analysis of the pipe-separator assembly. The convective velocity required to create coincidence is approximately [ ] times larger than the convective velocity that is considered in the FIV analysis.

For the higher modal frequencies of the pipe-separator assembly, higher convective velocities are necessary for the phase relationship between the forcing function and the structural mode shapes to become coincident. Because there is a large separation between the coincident frequencies and the natural frequencies of the pipe-separator assembly, the contribution to the coherence function from the phase and spatial relationship of the convective velocity is minimal. Any differences in the convective velocity used in this evaluation and the actual convective velocity that would be determined by instrumentation and testing of the primary steam separators would not have a significant influence on the FIV results reported in Section B.3.3.

Because it is not possible for the convective velocity to be higher than the mean free stream velocity through the steam separators, the assumption that the convective velocity is equal to the mean free stream velocity is conservative. Determination of the actual convective velocity through the use of dynamic pressure sensors installed in the pipe and separator assembly is not necessary. The spatial and phase relationship aspects of the convective velocity and its influence on the coherence of the forcing function with the flexural mode shapes of the pipe-separator assembly are conservatively evaluated. Determination of the actual convective velocity is not necessary to predict that the response of the pipe-separator assembly to turbulence due to the parallel flow through the assembly is acceptable.

Correlation Length

A correlation length of 0.4(R_H) is applied in the FIV analysis of the pipe-separator assembly. The larger the correlation length, the greater the coherence of the forcing function with the structural mode shapes and frequencies. The coherence range can not be larger than the characteristic length or the hydraulic radius of the flow channel. Even considering a correlation length equal to the hydraulic radius of the pipe-separator assembly (R_H), the response of the pipe-separator is determined to be small:

Max displacement (Node 90) = [ ] mil, rms

Max stress (Node 1) = [ ] psi, rms

No frequency or spatial dependence is assigned to the correlation length. Based on two different tests with annular axial flow, as described in Reference 4, Section 8.9, the correlation length is found to be fairly independent of the frequency and approximately equal to 40 percent of the annular gap width of the flow channel or 0.4(R_H). This assumption is not valid for low frequencies where the forcing function is dominated by acoustics. This is not the case for the FIV analysis of the pipe-separator assembly.

The spatial relationship of the correlation length and the influence of the correlation length upon the coherence between the forcing function and the flexural mode shapes do not exist for the flow conditions inside the pipe-separator assembly. The determination of the correlation length and its frequency dependence is not necessary to predict that the response of the pipe-separator assembly to turbulence due to the parallel flow through the assembly is acceptable.

Power Spectral Density (PSD) Function

The PSD applied in the FIV analysis of the pipe-separator assembly is acceptable for single phase flow applications in either industrial piping systems or confined annular flow without cavitation. As described in Reference 4, Section 8.9, this PSD derived from test data of a scale model test with annular flow and agrees with the data obtained from measurement on the full scale prototype. Reference 4 also explains that this PSD exhibits a much higher turbulence intensity for the same velocity when compared to other PSDs for piping systems (See Reference 4, Equation 8.68) because the flow in this test was allowed to impinge on the flow channels perpendicularly before it flowed down the annular flow channel. The flow was more turbulent compared to those over flat plates or in straight pipes. The PSD was developed experimentally from single phase flow tests, but the steam mixture in the separators is two-phase. It is generally accepted that the single phase PSD provides a greater energy distribution as a function of the frequency when compared to a two-phase PSD.

The PSD that is applied in the FIV evaluation of the primary steam separator is conservative. It is expected that the determination of the actual PSD in the primary steam separators through instrumentation with dynamic pressure sensors would not provide a PSD that would bound the

one currently used. The determination of this FIV input by full scale flow tests of the U.S. EPR RSG is not necessary to conservatively predict the response of this structure to turbulence due to the parallel flow through these components.

B.3.5 Conclusions

As stated in Section B.2, there are no operating RSG designs in Europe or the U.S. that employ the S 335-2 two stage primary steam separators. For this reason, the FIV analysis of the primary steam separators is performed to confirm the integrity of this component. The FIV results for the steam separators reported in Section B.3.3 for the parallel flow excitation through the primary steam separators predict a low response for these components. The maximum stress ([ ] psi, rms) and displacement ([ ] mils, rms) is determined, which both have a significant margin to the allowable values.

Because there is no practical means to create the design flow conditions in the steam generator without loading fuel into the reactor vessel (i.e., post hot functional testing), the determination of this unique data during HFT, as specified by Reference 1, to then be confirmed or reevaluated with the full scale analytical evaluation prior to startup testing is not feasible.

The integrity of the U.S. EPR RSG primary steam separators can only be verified through conservative analytical evaluations. Scale model and full-scale model tests and analytical evaluations and the instrumentation of the primary steam separator for HFT to acquire the full-scale PSD, the convective velocity, the correlation length, as well as other FIV inputs, is not necessary to demonstrate the FIV integrity of pipe-separator assembly. Considering the upper bound FIV inputs for the analysis of the primary steam separators, these structures are not susceptible to excitation created from turbulent parallel flow and will not experience excessive flow-induced vibrations.

B.4 FIV Evaluation of the RSG Steam Dryers

Historically, FIV related failures of steam dryers in BWR plant designs have been associated with conditions of acoustic resonance in the main steam piping systems. Using the criteria established in A.2.1 for predicting acoustic resonance, a methodology for screening the design of the piping systems attached to the U.S. EPR RSG is described in this section. This screening will verify that the piping systems are free from acoustic excitation and verify that the steam dryers will also be free from acoustic excitation. Evaluation of standoff pipes for the valves, standoff branch lines, or other cavities that have the potential to create acoustic resonance are evaluated in the design of main steam, main feedwater and the other piping systems attached to the RSG.

The failure of a steam dryer due to excitation from the turbulent steam flow through the dryers has not been observed. Based on the historical operating experience with nearly identical steam dryer designs, the improbability that the steam dryer will experience significant vibrations resulting from the excitation by random turbulence is justified in Section B.4.1.

Section B.4.2 provides the justification that the instrumentation and the acquisition of test data during HFT and the subsequent interpretation of this data, as specified by Reference 1, is not required to demonstrate the FIV integrity of the steam dryers.

B.4.1 Random Turbulence

The excitation of the steam dryers resulting from the turbulent flow through these components is addressed in this section. Based on the complex flow patterns through the steam dryers and the design of the dryer itself, rigorous evaluation of the steam dryers is difficult and the accuracy of the results would be questionable. The integrity of the steam dryers for excitation resulting from random turbulence is justified based upon the operating experience of the design of the steam dryers (STAR type).

As described in Section B.2.1, the steam exits the separators and enters the [ ] dryer cells arranged vertically in a STAR pattern. [ ] cells are arranged around the periphery and the other [ ] are located in a radial direction. Each dryer cell is constructed primarily from chevron-type dryer vanes which create directional change in the vapor to further separate the steam / water mixture.

As shown in Table B-1, the 79/19T and 73/19TE RSG designs employ the STAR steam dryer type design, which have nearly identical rectangular dimensions as the U.S. EPR RSG steam dryers. The materials used in the construction of the currently operating steam dryers are identical to the U.S. EPR steam dryers. The temperature and density of the steam in the steam drum is also approximately the same for these plants. These RSGs are theoretically the same, despite the differences in the rectangular dimensions of the dryer cells in these RSGs and the modal frequencies and eigenvectors for the steam dryers, considering the influence of the hydrodynamic mass of the steam.

As shown in Table B-1, the nominal flow rate through the dryer cells based on the rectangular dimensions at each of the operating plants bound the flow rate for the U.S. EPR RSG steam dryers. The nominal flow velocity through the U.S. EPR steam dryers is [ ] inch/sec. The nominal flow velocity through the 79/19T RSG dryer cells is [ ] inch/sec and [ ] inch/sec for the 73/19TE RSG designs to provide a lower and upper bound for the U.S. EPR RSG steam dryer design. The turbulent excitation of the steam flow through the dryer cells and across the chevron-type dryer vanes is similar among the operating and non-operating RSG designs.

Based on these comparisons, it is concluded that the integrity of the U.S. EPR RSG steam dryers to cross-flow random turbulent excitation is verified by the operating experience at the four European plants. The combined operating experience for the STAR steam dryers is more than 40 years. At least 12 years of operating experience have accumulated at two plants.

B.4.2 Justification for the Exceptions to RG 1.20 for the Steam Dryers

This section provides the justification that the instrumentation, the acquisition of test data during HFT, and the subsequent interpretation of this data, as specified by Reference 1, is not necessary to demonstrate the FIV integrity of the U.S. EPR RSG steam dryers.

The main steam, main feedwater, and the other piping systems attached to the RSG will be designed and analyzed with the criteria established in Section A.2.1 to verify that the RSG internals and piping system components will not experience acoustic resonance excitations. The main steam and main feedwater piping systems that are attached to the RSG will be instrumented with permanent sensors to measure and monitor pipe vibrations during startup testing and during the service life of the plant as shown in Appendix A. If unexpected vibrations resulting from acoustic resonance are observed in these piping systems during initial plant startup testing, these sources of excitation will be addressed and the piping will be redesigned as needed. This type of flow excitation has identifiable symptoms, including loud acoustic whistles and pipe vibrations, which the accelerometers attached to the piping systems will be capable of detecting during hot functional testing.

As concluded in Section B.4.1, the operating experience of the U.S. EPR RSG steam dryers (STAR type), in addition to the evidence that no incidences of steam dryer failures in steam generators with almost identical dryers, provides evidence that these components have acceptable performance and integrity regarding turbulent flow excitations.

Based on this justification, the scale and full scale model tests and analytical evaluations for a prototype design outlined in Reference 1 and the instrumentation of the steam dryer for HFT to acquire the full scale PSD, the convective velocity, the correlation length, and other FIV inputs is not required to demonstrate the FIV integrity of the steam dryers.

B.5 FIV Evaluation of the Other RSG Upper Internal Components

The recirculation ratio for the U.S. EPR primary steam separators and dryers is approximately [ ] as reported in Table B-1. Referring to Figure B-1, the recirculation flow is drained from the steam dryers in the upper internals through drain piping located in the periphery of the steam drum to an elevation just below the entrance to the steam separators. The majority of the recirculation flow from the steam separators is discharged from the first stage, which is located at the entrance to the separators as shown in Figure B-1.

Since most of the steam separator recirculation flow is discharged from the first stage, at the entrance to the separators, this flow cannot create flow excitation of the steam separator external surfaces. The external surfaces of the entrance piping, between the steam separators and the wrapper top, are exposed to the axial flow created by the steam separator recirculating flow. However, the magnitude of the axial flow is insufficient to create a significant response of the steam separator to turbulence. Because this flow is discharged vertically, there is no cross-flow component that could create a response of the steam separator to turbulence. The recirculation

flow discharged from the second stage of the primary steam separators is also small and cannot create significant steam separator flow excitation due to turbulence in the axial or cross flow directions. Although the distribution of the recirculation flow in the steam drum has not been determined, the velocity that would act on the steam separator external surfaces would be less than [ ] foot per second.

Evaluations for the secondary side flow excitation of the main feedwater distribution system, the emergency feedwater header rings, and the drain piping are performed and demonstrate that these components will not experience excessive flow-induced vibrations. These components were either screened or evaluated for flow excitation resulting from vortex-shedding, random turbulence due to cross flow condition, and acoustic resonance adhering to the analytical methods provided in other sections of this report.

Given the large flow area created by the boundary of the steam generator (SG) upper shell and the small magnitude of the single-phase recirculation flow, the SG upper internal components located in this region of the steam drum (the main feedwater distribution system, the emergency feedwater header rings) cannot experience significant flow excitation due to random turbulence from the recirculation flow. The location of the drain piping in the periphery of the steam drum, away from the steam separator exhaust, eliminates the possibility for this flow to create flow excitation of the drain piping due to random turbulence or vortex-shedding.

Although the secondary side mass flow rate for the US EPR steam generator SG is [ ] percent higher than the SG identified in Table B-1, the U.S. EPR SG upper internal components are not susceptible to significant flow excitation for the reasons identified in this section.

B.6 Conclusions

The integrity of the U.S. EPR RSG upper internals is verified by:

- Conservative analytical evaluations of the RSG upper internals.
- The operating experience of the steam dryers design (STAR type).
- Screening methods and design considerations of the piping systems attached to the RSG to verify that the conditions conducive to acoustic resonance in these piping systems is eliminated as a source of excitation to the RSG upper internals.
- Permanent instrumentation of the main steam and feedwater piping systems attached to the RSG to monitor pipe vibrations during startup testing and during the service life of the plant.

The results of the FIV evaluations for the full power, steady state, normal operating conditions demonstrate that these RSG upper internals are not susceptible to significant flow induced vibrations and have substantial margin to the acceptance criteria.

If unexpected vibrations resulting from acoustic resonance are observed in the attached piping systems during initial plant startup testing, the sources of excitation upon the RSG steam dryers (or any other RSG upper internal component) and piping systems will be addressed and the

piping will be redesigned if required. Flow excitation due to acoustic resonance has very identifiable symptoms of load acoustic whistles and pipe vibrations which the accelerometers attached to the piping systems will be capable of detecting.

These measures will confirm that the RSG upper internals will not experience excessive flow-induced vibrations. The scale and full scale model tests and analytical evaluations for a prototype design outlined in Reference 1 and the instrumentation of the upper internals for HFT to acquire the full scale PSD, the convective velocity, and the correlation length, as well as other FIV inputs, is not required to demonstrate the FIV integrity of the U.S. EPR RSG.

APPENDIX C: VIBRATION ASSESSMENT OF THE RSG TUBE BUNDLE

The Regulatory Guide 1.20 (Reference 1) does not provide guidance for the assessment of the FIV integrity of the SG tube bundles. The FIV analysis of the SG tube bundle is performed using the guidance of the 2004 ASME Boiler and Pressure Vessel (B&PV) Code, Section III, Appendix N-1300 (Reference 9(a)). The methodology and design inputs considered for the FIV analysis of the of the U.S. EPR steam generator (SG) tube bundle are described in this Appendix of the Technical Report.

C.1 Overview of FIV Analysis Methodology Performed for the RSG Tube Bundle

The following FIV mechanisms are evaluated for the U.S. EPR SG tube bundle:

- Fluid-elastic instability (Connors' mechanism).
- Cross-flow turbulence-induced vibration.
- Vortex-induced vibration.
- Parallel (Axial)-flow turbulence-induced vibration (primary and secondary side flow).

The FIV analysis evaluates the SG tube bundle for fluid-elastic instability and vibrations induced by random turbulence excitation and vortex shedding using traditional linear frequency domain techniques. The FIV analysis is performed for the design full power level (4590 megawatt thermal) steady-state, normal operating conditions considering the secondary-side flow conditions resulting from fouled tubes (design fouling of [ ]) and 10 percent of the tubes plugged. To account for uncertainties in the primary flow measurements, the secondary side thermal-hydraulic inputs to this FIV analysis includes an additional [ ] MWth of primary fluid heat.

The worst-case tube locations are evaluated based on the tube support configuration and the secondary side thermal-hydraulic profiles. Specifically, the tubes with the longest spans between anti-vibration bars are analyzed. The in-service virgin tube condition (i.e., un-corroded) and tubes with 40 percent TW (through-wall) wear flaws are evaluated. The thermal-hydraulic profiles, including the secondary side fluid densities, fluid velocities, and void fractions, are reviewed to confirm that bounding dynamic pressures are analyzed for each tube support configuration.

The computer program AutoFIV is used to perform the FIV analysis on the U.S. EPR SG tube bundle. The AutoFIV program integrates the various software applications that are used to perform FIV analysis of SG tubes into a single analysis system with a single input file, streamlining the analysis process. AutoFIV acts as an executive program, generating the input files for the various analysis applications, directing their execution, managing the flow of data between the applications, and consolidating the output. The AutoFIV integrates the following applications:

- CASS Preprocessor: generates the finite element models (FEMs).
- CASS HPE Stress: generates the eigensolutions.
- PCSTAB2: performs the fluid-elastic stability analysis.
- PCRANDOM: performs turbulence and vortex-induced random vibration analysis

The analytical methodology employed by these software codes is described in Sections 4.3.2.1.1, 4.5.1.1.1, 4.5.1.1.3, and 4.5.1.1.4 of this Technical Report.

The modal analyses for the tubes selected for evaluation includes the hydrodynamic mass of the primary and secondary side fluid. The added mass coefficient for a tube within the SG tube bundle is calculated as [ ] through the relationship in Reference 2, Table 2-2, Case 7, and provided below:

$$M_c = \frac{(D_e/D)^2 + 1}{(D_e/D)^2 - 1} \quad \text{with} \quad D_e/D = (1 + P/2D)P/D$$

Where:

P is defined as the tube pitch.

D is defined as the tube OD.

P/D is the pitch to diameter ratio.

The first 60 modal frequencies for each of the limiting tube locations are determined and evaluated for each of the four FIV mechanisms identified above. The cutoff frequency for each tube location is related to the geometry and boundary conditions of the tube and the u-bend radius. The first 60 modal frequencies results in a cutoff frequency of approximately 140 Hz for the largest u-bend radius tube and 165 Hz for the smallest u-bend radius tube.

C.2 Flow and Vibration Test Models

The U.S. EPR SG tube bundle has a [ ] inch triangular pitch tube arrangement with 0.75 inch OD x 0.043 inch wall tubes. AREVA NP has performed flow tests to determine the Connors' constant for SG tube bundle designs that are similar to the U.S. EPR SG. Tests were also performed to determine the inclusive damping ratio, which considers damping associated with non-linear tube to tube support plate (TSP) interactions and secondary side fluid effects. The Connors' constant is derived from empirical data collected during experiments and mockup tests, particularly the SRM and EVA tests. Results of these tests are provided in EPRI Report NP-4559 (Reference 26) and the EPRI SG Reference Book (Reference 27).

The ASME Section III, Appendix N-1331.2, 2004 guidance recommends values of 4.5 and 4.0 respectively for the triangle and rotated triangle tube arrangements with P/D ratios between 1.25 and 1.5. Based on conservative values determined from the experimental results reviewed in

References 26 and 27, a Connors' constant (β) equal to [ ] is determined for straight tube sections. For the u-bend region, a value of [ ] for the Connors' constant is determined. These values for the Connors' constant are equal to, or bound, those values recommended by the ASME Code.

These inputs for the fluid-elastic instability analysis of the U.S. EPR SG tube bundle are derived from the following tests.

C.2.1 EVA I Mockup Test and Results:

The EVA I mockup consists of a cylindrical pressure vessel that is vertical. The fluid flows upward through the vessel and then into a channel where three distinct sets of identical, straight 0.75 inch OD x 0.043 inch wall tubes were tested. These include a single tube, a row of ten tubes, and a rectangular bundle with a 1.08 square pitch involving six rows of ten tubes each. These tests were performed to determine the Connors' constant for straight tube sections for a variety of flow conditions.

The EVA I tests conclusions summarized in Reference 26, Section 3.5.3 shows that a Connors' constant of 7.2 was determined for two-phase flow, and a Connors' constant of about 4.5 for a single phase flow condition. Reference 26, Figure 3.5.3-1 provides the stability diagram for the EVA I flow tests. Reference 26, Figures 3.5.3-2 through 3.5.3-4 compares these results to other industry data. ASME Code Section III, 2004, Appendix F, Figure N-1331-4 compares the Connors' constant for 170 data points.

As noted in Reference 26, Section 3.5.3.1, the validity of the Connors' constant value of 4.5 for the in water flow is uncertain at the low values of reduced damping (A_R = 0.12) with the Connor's model. Because low reduced damping (e.g., $m(2\pi\zeta)/\rho D^2 < 0.7$) prevails in heavy fluids such as water, the instability mechanism is controlled by the fluid velocity mechanism (fluid-damping-controlled). In this case, fluid coupling is not necessary to cause instability of a tube. For flow conditions where low reduced damping exists, ASME Code Section III, Appendix N-1331.2, 2004 states that "neither the theory nor test data are sufficient to establish values of the C" (Connors' constant), and recommends a value of 3.3 for the Connors' constant.

Because the flow conditions at the entrance to the tube bundle (i.e., the first span) of the U.S. EPR SG tube bundle are two-phase, the Connors' constant value of 4.5 determined for single phase flow conditions is not applicable. A conservative Connors' constant value of 3.0 is used with the fluid-elastic instability analysis of the straight tube sections of the tube bundle and bounds the recommended value of 3.3 prescribed by the ASME Code when low reduced damping, indicative of single phase flow conditions, prevails.

C.2.2 EVA II Mockup Test and Results:

The EVA II mockup consists of a cylindrical pressure vessel with a nominal diameter of 27.6 inches that are closed at both ends by ellipsoidal heads. Eighty U-tubes (eight rows of ten tubes

each) are installed in a 1.08 inch square pitch pattern. Tube OD is 0.750 inch with a wall thickness of 0.043 inches. The straight section length for each tube is 86.7 inches. The smallest u-bend radius is 2.95 inches and the largest is 12.67 inches. Two quatrefoil-broached TSPs are installed in the test section at 40.87 inches and 81.73 inches above the tube sheet (TS). The five rows of u-bend sections are fixed by anti-vibration bars (AVB).

Although the EVA II testing do not specifically determine the Connors' constant for the u-bend tube region of the tube bundle, no fluid-elastic instability is observed at the flow conditions that are investigated. These tests are performed to determine the inclusive damping ratio. This damping ratio is inclusive of the fluid damping and the damping resulting from tube-to-TSP interactions for small amplitudes of vibrations that are typically associated with random turbulence and the interaction between the tube and TSP.

Reference 26, Section 5.3.4 states that "damping factors of a few percent were observed in two phase flow." Reference 26, Section 4.2.3 and Figures 4.2.3-1 through 4.2.3.4 provide the detailed results of these damping tests. The damping factors determined from these tests are representative of small amplitudes of vibrations where it is probable that not all TSPs are active in supporting the tube. These damping factors are not representative of the damping experienced by a tube at the onset of fluid-elastic instability when large amplitudes of vibrations that are typically prevalent at sub critical flow velocities. The FIV analysis for random turbulence applies a viscous damping ratio of 1 percent (see Section C.4.1.2).

In-air damping tests to assess the damping ratio associated with the large amplitudes of vibration that are characteristic of fluid-elastic instability are not included in the test campaign described herein. ASME Code, Appendix N-1331.3 suggests a 1 percent damping ratio for tightly supported tubes, which is indicative of locked TSP conditions where the buildup of secondary side corrosion products between the tube and TSP crevices reduces the clearance between the two components, reducing the damping. The buildup of the corrosion products associated with drilled carbon steel TSPs is not predicted to occur with the broached, stainless steel TSP design of the U.S. EPR SG tube bundle. These values of damping are inappropriate for application to the U.S. EPR SG tube bundle.

AREVA NP has performed in-air damping tests to assess a damping ratio for analysis of fluid-elastic instability. Damping tests performed for re-circulating tube bundles and once through tube bundles have consistently shown a damping ratio of at least 3 percent. Reference 25 reviews the methods of determining a damping ratio used by AREVA NP, as well as the results of damping tests performed for a once through SG. Reference 25 also provides an executive review of the damping ratios for other SG vendors. Additional evidence for the 3 percent damping ratio, indicative of a loosely supported tube, is conservatively recommended by Reference 4, Table 7.4. The damping ratio characterized by the onset of fluid-elastic instability could be 5 percent or more as stated in ASME Code, Appendix N-1331.3. For U.S. EPR SG, a conservative damping ratio of [ ] is applied to the straight and u-bend tube sections for

the analysis of fluid-elastic instability. The hysteresis damping (~0.5 percent for alloy 690) of the tube material is included in this [ ] damping ratio.

C.2.3 SRM Test Results:

The results of the SRM test program are described to add additional credence to the EVA tests for the Connors' constant. The SRM test campaign was performed prior to the EVA tests to investigate the fluid-elastic instability mechanism in the u-bend region of the tube bundle. The dimensions of the U-tube model used in the SRM tests are identical to the EVA test program.

Reference 26, Section 4.3.2 states that fluid-elastic instability was observed in the u-bend region in the out-of-plane direction with a natural frequency of 22 Hz in flowing water. For the single phase flow regime, the reduced damping was about 0.5 and the Connors' constant (β) is determined to be about 6.5. As stated in Section C.2.1, the validity of the Connors' model with low reduced damping is questionable. Due to this uncertainty, a supplementary margin is applied and a Connors' constant equal to 4.0 is selected for analysis of the u-bend region of the tube bundle. This value is in accordance with the recommendations of the ASME Code.

C.2.4 Summary of FIV Inputs Derived from Tests

Conservative values for the Connors' constant [ ] for straight tube sections and [ ] for the u-bend region, which are either equal to or bound the ASME recommended values, are applied in the analysis of the SG tube bundle for fluid-elastic instability.

A viscous damping ratio of [ ] representative of the damping associated with the hysteresis of the tube material and the tube-to-TSP interactions is applied to the analysis for fluid-elastic instability. This damping ratio bounds typical values of damping that have been determined with in-air damping tests (3 percent) and the damping estimated by the ASME Code during the onset of fluid-elastic instability (5 percent) and is conservative.

C.3 Analysis for Fluid-elastic Instability

The methodology used for the U.S. EPR SG tube bundle evaluation for fluid-elastic instability is identical to the method described in Section 4.5.1.1.3 for the column supports. The eigenvalue and eigenvector solutions are obtained by the method described in Section C.1. A review of the design inputs for this FIV mechanism unique to the U.S. EPR SG tube bundle is provided in the following sub-sections.

C.3.1 Analysis Inputs

C.3.1.1 Connors' Constant

A Connors' constant of [ ] is applied to the straight tube sections of the tube bundle and a Connors' constant of [ ] is applied to the u-bend region. These values represent

conservative values for the Connors constant based on mockup testing and ASME Code recommendations as summarized in Section C.2.4.

C.3.1.2 Damping

Damping Due to Tube-to-Tube Support Plate Interaction

The damping ratio that is applied in the fluid-elastic instability analysis accounts for the non-linearity of the clearance between the tube and the tube support and the capacity of the structure to dissipate energy. For fluid-elastic instability analysis (large vibration amplitudes at instability or at the threshold of instability), a [ ] damping ratio is applied to the hot leg and cold leg straight tube segments for the design condition in which the tube supports behave as pinned boundary conditions. A damping ratio of [ ] is applied to the u-bend regions. The hysteresis damping (~0.5 percent for Alloy 690) of the tube material is included in this [ ] damping value. These conservative damping values are based on the mockup testing summarized in Section C.2.4

Damping Due to Two-Phase Fluid

For the secondary side, a two phase fluid damping ratio is based on industry data (References 21 through 23). An additional 2 percent damping is credited to the damping ratio for tube elevations where the void fraction is between 60 percent and 90 percent.

C.3.2 Acceptance Criteria:

A fluid-elastic stability margin (FSM) greater than 1.0 implies that the tube bundle is stable, while an FSM less than 1.0 implies that the tube bundle will become unstable. For the U.S. EPR SG, a conservative acceptance criterion for fluid-elastic instability of FSM greater than [ ] is used, which represents a margin of safety [ ] percent. The acceptance criterion applied to the U.S. EPR tube bundle for fluid-elastic instability is identical to that provided in Section 4.5.2.1 for the column supports but is provided in Table C-1 for completeness.

C.3.3 Summary of Results for Fluid-elastic Instability

The minimum computed FSM are summarized in Table C-2 for the bounding tube locations. The minimum FSM of [ ],which occurs in the top span of the cold leg for a column [ ] tube location, is above the minimum allowable FSM of [ ].

C.4 Analysis for Random Turbulence due to Cross Flow Conditions

The methodology used to evaluate the U.S. EPR SG tube bundle for random turbulence induced vibration due to cross flow condition is the same methodology described in Section 4.5.1.1.4 for the support columns. The eigenvalue and eigenvector solutions are obtained by the method

described in Section C.1. A review of the design inputs for this FIV mechanism that are unique to the U.S. EPR SG tube bundle is provided in the following sub-sections.

C.4.1 Analysis Inputs

C.4.1.1 Forcing Function (PSD, Correlation Length, Convective Velocity)

Power Spectra Density Function

The power spectral density (PSD) applicable to the flow excitation resulting from random turbulence of the tube bundle due to cross flow conditions is identical to that provided in Figure 4-34, which is reproduced in Figure C-1. This empirical relationship for the single-phase PSD, as proposed by Pettigrew and Gorman (Reference 24) and as recommended by ASME Code Section III, Appendix N-1300, Figure N-1343-1 is applied to the tube. The upper bound frequency limit in Figure C-1 is increased to illustrate that the range of modal frequencies that are evaluated are bounded by the frequency range of the PSD.

The empirical formula for the two-phase PSD, as given by Pettigrew and Taylor (Reference 22), is lower than the corresponding single-phase PSD for the same dynamic head. In Figure C-2, these normalized PSDs are plotted against a backdrop of additional test data and against empirical equations recommended by various sources. The two PSDs in Figure C-2 that would be computed by Reference 24 at the fixed pitch velocity of 120 in/sec (at different frequencies) and at a fixed frequency of 50 Hz (at different pitch velocities) are plotted for comparison to the other PSDs. With the exception of the "vorticity-active" range, the equation in Reference 24 gives more conservative PSD for nuclear SG applications. AREVA NP applies the more conservative single-phase PSD (Reference 24) to the entire tube for the following reasons:

- The equation in Reference 24 is based on test data pertinent to nuclear SGs, with most of the data from water-based experiments with pitch velocities and tube frequencies concerning nuclear applications. More recent tests are in-air tests with higher tube natural frequencies than are typical in nuclear SG applications.
- The equation in Reference 24 is more conservative, except in the "vorticity-active" range, which is addressed later in the response for vortex-shedding excitation.

Correlation Length

The correlation length (λ) along the length of the tube is set equal to [ ] of the tube. The forcing function is considered completely coherent in the width direction of the tube.

Convective Velocity

The convective velocity is equal to approximately [ ] of the cross flow gap velocity, but the tube responds to a forcing function that is completely in-phase because the wave front arrives at the points along the tube at the same time.

C.4.1.2 Damping

For the in-plane and out-of-plane directions, a [ ] total viscous ([ ] structural) damping ratio is applied to the entire tube, disregarding the two-phase damping. This damping value is assigned to the whole tube and is representative of the damping due to the non-linear interaction of the tube and TSP with small amplitude vibrations and the damping associated with hysteresis, which is typically about 0.5 percent for Alloy 690 tube materials. This damping ratio includes the following damping mechanisms, which have a negligible contribution to the total damping:

- Damping due to the viscosity of the steam or fluid.
- The squeeze film damping.

C.4.2 Acceptance Criteria

C.4.2.1 For Displacements

The displacement acceptance criterion applied to the U.S. EPR SG tube bundle for random turbulence induced vibrations is identical to that provided in Section 4.5.2.2 for the column supports. The specific value for the acceptance criterion that is applied to the SG tube bundle is provided in Table C-1. This value represents the minimum tube displacement that could result in tube-to-tube impact, considering a five sigma (5σ) probability and half the gap clearance between the adjacent tubes. A five sigma (5σ) probability is representative of approximately a 100 percent probability that the allowable displacement will not be exceeded.

One half of the gap clearance between adjacent tubes is [ ] inch and provides an allowable displacement of [ ] inch, rms. The predicted rms displacement must be less than the acceptance criterion. The application of this acceptance criterion to the u-bend displacements is conservative because the criterion does not account for the tube indexing in the u-bend where the vertical clearance or pitch between the adjacent tubes is larger than the pitch in the straight sections of the tube bundle.

C.4.2.2 For High Cycle Fatigue

The criterion established in Section 4.5.2.2 is applied to the U.S. EPR SG tube bundle. Because the $P_L + P_b + Q$ stress range is below 27.2 ksi and the mean tube stress is low, fatigue curve "A" is applicable to the u-bend sections and the straight tube sections, except as noted below for the first span. The allowable stress is [ ] at 10^{13} cycles.

The tube material at the hydraulic expansion in the tubesheets could have a residual stress near the yield strength of the tube material. Therefore, fatigue curve "C" is applicable near the tubesheet in the first span. The allowable stress from fatigue curve "C" of [ ] at 10^{13} cycles was applied to the stresses at the secondary face of the tubesheet on the hot leg and cold leg.

C.4.3 Summary of Results

The displacement results of the random turbulence-induced vibration analysis are provided in Table C-3. The ratios of the displacements to the allowable displacement are calculated. A ratio of displacement to allowable displacement that is less than 1.0 indicates that the displacements for that bounding tube location are acceptable.

The ratio of the displacement to the allowable displacement does not account for the tube index in the u-bend. The tubes that are located in tube columns less than [ ] do not have tube indexing, and the straight tube length for these tube locations are identical. The tubes located in columns [ ] through [ ] have tube indexing. The straight tube length in these tube columns increases as the column number increases. Indexing the tube increases the in-plane radial gap clearances in the u-bend between adjacent tubes and has the effect of decreasing the gap velocities in the u-bend when compared to a tube bundle without tube indexing. For the tubes in columns [ ] through [ ], the clearance in the u-bend varies as a function of the u-bend angle and reaches the maximum clearance at the top of the u-bend. Tube indexing does not increase the clearance between adjacent tube locations in the u-bend for the out-of-plane direction.

Because there is an additional clearance due to the tube index in the u-bend for tubes in columns [ ] through [ ], the displacement acceptance criteria is conservative for these tube locations. The results are acceptable for the tube locations except for the in-plane displacements for column 113. For the column 113 tube location, the ratio of the maximum in-plane u-bend displacement to the conservative allowable displacement (1.25) does not account for the tube index. Additional calculations are preformed to demonstrate the acceptability for the in-plane u-bend displacements for this tube location.

A node-specific allowable in-plane u-bend displacement is calculated that accounts for the tube index. The rms response of the tube is provided in the rotated nodal coordinate system. Only the DOF1 (nodal "x" axis) responses are compared to the allowable perpendicular displacement for each node in the u-bend. For a column 113 tube only, the u-bend in-plane responses in the first degree of freedom are compared to the node-specific allowable displacements listed in Table C-5, which shows that the u-bend in-plane displacements for a column 113 tube are acceptable.

The resulting tube moments due to random turbulence-induced vibration are taken from the computer output files and the corresponding stresses are calculated using the section modulus of the unflawed and flawed tube sections. The resulting stresses are summarized in Table C-4 for the unflawed tube. As shown in Table C-4, the resulting stresses are below the allowable stress limits. The maximum stresses in the flawed tube were determined for the limiting TSP and AVB tube support locations. The section modulus for a wear flaw that may occur at a TSP conservatively assumed a wear flaw at each of the three lands of the TSP. For the AVB tube support locations, the section modulus of a flawed tube is determined with two opposing wear

flaws. The wear flaws are modeled with a depth of 40 percent through-wall, which represents the typical plugging limit for tube wear at supports in U.S. SGs. The maximum stress in flawed tubes is calculated as:

$$\sigma_{FlawedTube} = FSRF * \sigma_{VirginTube} \left(\frac{Z_{VirginTube}}{Z_{FlawedTube}} \right)$$

where a conservative fatigue strength reduction factor (FSRF) of [ ] is applied. The ratio of the section modulus terms $\left(\frac{Z_{VirginTube}}{Z_{FlawedTube}} \right)$ adjusts the stress computed for the virgin tube to that of the flawed tube. The section modulus term (Z=I/c) is the ratio of the area moment of inertia to the radius of the stress fiber where the stress is computed.

Table C-6 provides the stress calculation results for flawed tubes. The maximum stresses are below the allowable stress of [ ].

C.5 Analysis for Random Turbulence Induced Vibration due to Parallel Flow Conditions

The surface pressure fluctuations that excite a SG tube in axial flow result from local turbulence created by the shear flow in the developing boundary layer and the free stream turbulence caused by upstream disturbances from the TSP. Parallel flows do not ordinarily cause failure of heat exchanger tubes because the tube stiffness is sufficient to prevent a parallel flow-induced instability. Turbulence-induced vibration due to parallel flow is important only when the following conditions exist:

- Where a tube severance exists, the only excitation mechanism is axial flow.
- The axial flow velocity is much higher than the cross-flow velocity in similar spans and is not bounded by a corresponding vibration analysis due to cross-flow.

The first condition does not exist in the U.S. EPR SG. However, the vibration response due to turbulent parallel (axial) flow is evaluated because the vertical flow is higher than the cross-flow velocity in similar spans at some locations.

Parallel flow relative to the tube axis occurs on both the primary side and the secondary side of the straight leg sections of the U.S. EPR SG. The maximum secondary side vertical fluid velocity of [ ] inch/sec occurs in a column [ ] tube. This secondary side flow velocity is approximately twice the velocity of the primary side parallel flow. Only the secondary side flow is evaluated for the vibration induced by random turbulence due to parallel flow and the results are considered bounding of the effects due to primary side flow.

The analysis methodology by which the U.S. EPR SG tube bundle was evaluated for FIV resulting from random turbulence due to parallel flow condition is provided in Section 4.3.2.1.

The eigenvalue and eigenvector solutions are obtained by the method described in Section C.1. A review of the design inputs for this FIV mechanism that are unique to U.S. EPR SG tube bundle are provided below.

C.5.1 Analysis Inputs

C.5.1.1 Forcing Function (PSD, Correlation Length, Convective Velocity)

Power Spectral Density Function

A PSD developed for single phase parallel flow within the fuel assembly of the reactor pressure vessel (RPV) is conservatively used for the two phase flow condition prevalent on the secondary side of the tube bundle. The dimensional pressure PSD is calculated by multiplying the dynamic pressure term computed at each node of the tube model by a frequency dependent random lift coefficient ($C_p(f)$) in the same way that the cross flow PSD is used to evaluate flow excitation resulting from random turbulence due to the cross flow conditions in the tube bundle. The random lift coefficient for the PSD is equal to;

[ ]

The $C_p(f)$ reported here [ ] is small in comparison to the typical design value of 0.025 from 0 to 40 Hz (see Figure C-1) used in the analysis of SG tube bundles for cross-flow conditions.

Convective Velocity

For parallel flow, the convective velocity is typically a large fraction of the mean or free-stream velocity. For this case, the convective velocity is set to a conservative value of 100 percent of the average parallel velocity for the span.

Correlation Length

The correlation length (λ) for external parallel flow in a tube bundle is:

$\lambda = 0.2\ P\ (1+ P/2D)$ (Per Reference 4, Equation 8.64).

Considering the pitch and tube diameter of the tube bundle, the computed value for the correlation length is equal to [ ]. The generalization for cross flow that larger correlation lengths produce larger responses cannot be applied to axial flow. If a particular turbulent eddy in axial flow persists longer than the dominant period of the adjacent structural vibration, then it may start to cancel out its own earlier influence. A conservative correlation length is determined by parametrically evaluating a range of correlation lengths and then comparing the resulting response to define a correlation length that creates the maximum response in the tube. A correlation length of [ ] inches is subsequently used in the analysis for turbulence resulting from parallel flow.

C.5.1.2 Damping

The damping ratio applied to the analysis for random turbulence due to parallel flow is the same as that described in Section C.4.1.2 for flow excitation resulting from random turbulence due to cross flow conditions. The viscous damping created by the parallel flow along the length of the tube, which increases with velocity, is conservatively ignored.

C.5.2 Acceptance Criteria

The acceptance criteria for displacements and stresses are the same as those described for the analysis for random turbulence induced vibrations due to cross flow conditions (Section C.4.2) and is provided in Table C-1.

C.5.3 Summary of Results

The displacement results of the random turbulence-induced vibration analysis for secondary side parallel flow are provided in Table C-7. The ratio of the displacement to the allowable displacement is calculated and a ratio of displacement to allowable displacement that is less than 1.0 indicates that the displacements for that bounding tube location are acceptable.

The resulting moments due to random turbulence-induced vibration for secondary side parallel flow are taken from the PCRANDOM output files and the corresponding stresses are calculated. The resulting stresses summarized in Table C-8 are below the allowable stress limits.

As shown in Table C-7 and Table C-8, the displacements and stresses associated with excitation caused by secondary side parallel flow are insignificant compared to the displacements and stresses associated with excitation caused by secondary side cross flow that are reported in Table C-3 through Table C-6.

C.6 Analysis for Vortex-Shedding Induced Vibration due to Cross Flow Conditions

As shown in Figure C-2, the PSD has a broad peak that is indicative of "vorticity activity" for fD/V_p between 0.1 and 0.7. Within this range, the PSD is about 20 times higher than that immediately outside of this range. A separate analysis is performed to address vortex-induced vibration.

Following the recommendations of ASME Code, Appendix N-1344, the turbulence-induced vibration technique is used, but with the PSD increased by a factor of 20, and a correlation length of 1000 inches is applied to simulate the fully coherent forcing function associated with vortex lock-in.

C.6.1 Analysis Inputs

C.6.1.1 Forcing Function (PSD, Correlation Length, Convective Velocity)

Power Spectral Density Function

The PSD provided in Figure C-1 is applied to the entire tube for the analysis of vortex-induced vibration. For the first span, this PSD is increased by a factor of 20 for the modal frequencies influential to the response of the tube in the first span of the cold leg and first span of the hot leg that fall within the broad peak shown in Figure C-2. From this figure, the "vorticity" active peak covers the range where the dimensionless frequency (fD/V) is equal to 0.1 to 0.7. The frequencies that fall within this range are calculated based on the average and maximum fluid velocities in the first span of the cold leg and the first span of the hot leg for the peripheral tube location with the highest dynamic pressure term.

The frequencies in the range of "vorticity" activity are compared to the modal frequencies that are influential in the first span. The PSD provided with Figure C-1 is edited by multiplying the lift coefficient in these frequency ranges by a factor of 20 to provide the PSD that is applied in the first span (See Figure C-3). The lift coefficient provided in Figure C-1 and Figure C-3 is in units of $(1/sec)^{1/2}$. The lift coefficient, as defined in these figures, is squared and multiplied by the square of the dynamic pressure term to provide the pressure PSD or $G_p(f)$ as reported in Section 4.5.1.1.4. The lift coefficient in units of (1/sec) is multiplied by the factor of 20. Therefore, the lift coefficient in Figure C-3 has a factor of $\sqrt{20}$ in the range of frequencies in the first span that are susceptible to "vorticity" activity.

Correlation Length

The correlation length in the first span is set to a large value of 1,000 to create a completely coherent forcing function in this span, which is consistent with the strongly coupled fluid-structure interaction that is associated with this FIV mechanism.

C.6.1.2 Damping

The vibration amplitudes that are associated with vortex-induced vibrations are of a similar magnitude to fluid-elastic instability. The damping values described in the Section C.3.1.2 are used for the vortex-induced vibration analysis (i.e., [ ] viscous or [ ] structural). This damping ratio is representative of the damping due to the non-linear interaction of the tube and tube support plate and the damping associated with hysteresis, which is typically about 0.5 percent for Alloy 690 tube materials, and conservatively ignores the damping associated with a two-phase mixture. For the vortex-induced vibration analysis, as described for the turbulent analysis, only one spatial damping value is applied along the entire tube length.

Because the PSD for vortex-shedding and the damping ratio applicable to the first span are applied conservatively to the entire length of the tube in the structural model, the computed results for vortex-shedding analysis are only applicable to the first span of the tube bundle.

C.6.2 Acceptance Criteria

The computed rms response for the tubes from the PC program "PCRANDOM" are converted to a zero-to-peak response by multiplying the rms response by the $\sqrt{2}$ for comparison to the allowable displacement and fatigue stress curves as described in the following sections.

C.6.2.1 For Displacements

One-half the gap clearance between tube locations is [ ] inch. Therefore, [ ] inch, 0-peak, is the acceptance criteria to prevent tube impacts between adjacent tubes for vortex-induced vibration.

C.6.2.2 For High Cycle Fatigue

The stress due to high cycle fatigue associated with flow excitation due to vortex-shedding is compared to the ASME fatigue curve "C" for austenitic steels presented in Figure 4-21 (zero to peak fatigue curve). The allowable stress at 10^{13} cycles is 13,200 psi (0-peak). Curve "C" is used because the maximum stress occurs in the first span at the secondary face of the tubesheet where residual stress from the hydraulic expansion is present.

C.6.3 Summary of Results

The results for a column 113 tube are summarized in Tables C-9 and C-10.

C.7 Analysis for RCP Acoustic Pressure Fluctuations

The RCS primary coolant pumps generate acoustic pressure fluctuations that propagate through the primary piping system and potentially into the SGs and impinge upon the tubes. The frequency of these pressure fluctuations depends on the RCS pump shaft rotational frequency and the number of pump blades. The first blade passing frequency is equal to the number of blades multiplied by the shaft rotation frequency. In most pumps, the most predominant pulse occurs at the first, second, or third blade passing frequency. These pulses are harmonic forcing functions with well-defined frequencies.

The U.S. EPR RCP is a single speed pump that operates with a design speed of 1200 rpm and has [ ] blades. The blade passing frequency is [ ] Hz. The average primary fluid temperature is 594°F and the primary side pressure is 2248 psia. The speed of sound in the primary fluid is 2902 ft/sec and the resulting wave length is:

[ ]

The largest amplitude and resulting acoustic pressure occurs with the first blade passing frequency. The harmonic acoustic pressure wave will vary between -ΔP/2 and +ΔP/2 in a distance of [ ] inches. Conservatively assuming 5 psi pressure fluctuations (ΔP), the pressure differential is on the order of ΔP/ [ ] per inch or [ ] psi/inch across the axial length of the tube (~ [ ] inches of straight tube length). The response of the tube to this pressure differential at this high frequency is insignificant.

Given the number of tubes with different u-bend radii and the closely-spaced frequencies typical of tube bundles, it is probable that a tube location would exhibit a coincident frequency to the RCP blade passing frequency of [ ] Hz. However, significant excitation of the tube due to this pressure fluctuation is not possible as described above. Additionally, the higher order mode shape of the tube at a frequency of [ ] Hz is incompatible with the shape of the pressure wave propagating along the length of the straight tube section for the blade passing frequency of [ ] Hz or its second or third harmonics. Tube locations that exhibit coincident frequencies to the RCP blade passing frequencies will not experience significant excitation from this source. The effects of these acoustic pressure fluctuations upon the vibratory behavior of the SG tube bundle are negligible.

Table C-1—Acceptance Criteria for FIV Analysis of the U.S. EPR SG Tube Bundle

Table C-2—Summary of Fluid-Elastic Instability Analysis Results

Table C-3—Summary of Displacements due to Random Turbulence-Induced Vibration for Cross Flow

(Sheet 1)

Table C-3—Summary of Displacements due to Random Turbulence-Induced Vibration for Cross Flow

(Sheet 2)

[
]

Table C-4—Summary of Stress due to Random Turbulence-Induced Vibration for Cross Flow

(Sheet 1)

Table C-4—Summary of Stress due to Random Turbulence-Induced Vibration for Cross Flow

(Sheet 2)

Table C-5—In-Plane U-bend Displacements for Column 113 on a Nodal Basis

Table C-6—Maximum Stresses for Flawed Tubes Resulting from Cross-Flow Turbulence-Induced Vibration

[

]

Table C-7—Summary of Displacements Due to Random Turbulence Induced Vibration for Parallel Flow

[

]

Table C-8—Summary of Stresses Due to Random Turbulence-Induced Vibration for Parallel Flow

Table C-9—Displacements Due to Vortex Shedding Induced Vibration

Table C-10—Stress Due to Vortex Shedding Induced Vibration

Figure C-1—Random Lift Coefficient for Random Turbulence due to Cross Flow (Per Reference 24)

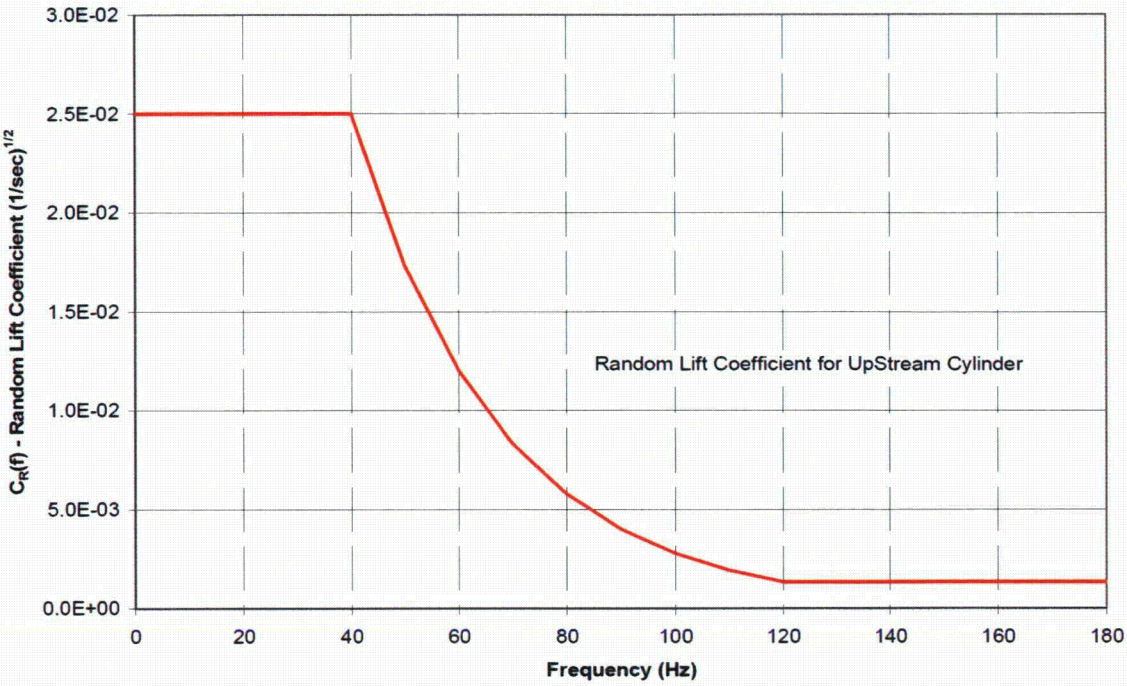

$C_R(f) = 10^{(af + b)}$.

$= 0.025$ for $f < 40$ Hz.

$= 0.00133$ for $f \geq 120$ Hz.

and

$a = -15.92E-03$.

$b = -965.4E-03$.

Figure C-2—Empirical Equations for the Random Pressure PSD (Recommended by various authors per Figure 9.5 of Reference 4)

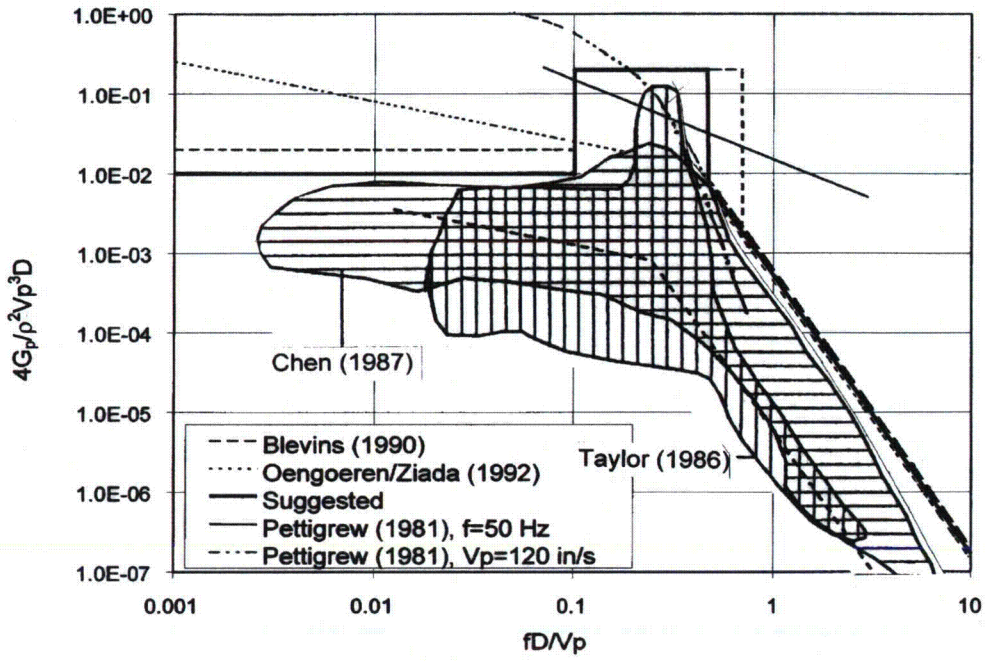

Figure C-3—Random Lift Coefficient for the Analysis of Vortex-Shedding